ADDIS ABABA UNIVERSITY

SCHOOL OF GRADUATE STUDIES

FACULTY OF TECHNOLOGY

DEPARTMENT OF CIVIL ENGINEERING

ASSESSMENT OF EARTHQUAKE ANALYSIS METHODS OF INTAKE TOWERS

A thesis submitted to the school of Graduate Studies in Partial fulfillment of the Requirements for the Degree of Master of Science in Civil Engineering (Structures)

By

MOHAMMED ABDULKADIR

Advisor: **Dr.-Ing. Adil Zekaria**

ADDIS ABABA UNIVERSITY
SCHOOL OF GRADUATE STUDIES
FACULTY OF TECHNOLOGY
DEPARTMENT OF CIVIL ENGINEERING

ASSESSMENT OF EARTHQUAKE ANALYSIS METHODS OF INTAKE TOWERS

By
MOHAMMED ABDULKADIR

OCTOBER 2011

Approved by Board of Examiners

Dr.-Ing. Adil Zekaria Advisor	_____ Signature	_____ Date
_____ External Examiner	_____ Signature	_____ Date
_____ Internal Examiner	_____ Signature	_____ Date
_____ Chairman	_____ Signature	_____ Date

ACKNOWLEDGMENT

I'm deeply indebted to Dr.-Ing. Adil Zekaria, Associate Professor at the Department of Civil Engineering, Adiss Ababa University, whose guidance and support has paramount importance in the completion of this thesis.

I would like also to extend my indebtness to Water Works Supervision Enterprise for finically and technically helping me to accomplishment the goals of the thesis. Also, my especial appreciation goes to Ato Kassahun Luliseged, Head of Water Works Supervision Enterprise; Ato Mohammed Ebrahim, Head of Design Core Process; and my colleagues working at Kesem Dam Irrigation project site.

In addition, I would like to express my gratitude to Construction Material Laboratory in Construction and Design Share Company for its whole-hearted collaboration while conducting laboratory test whose results served as in put for carrying out the study.

TABLE OF CONTENT

ABSTRACT

Seismic analysis of an intake tower may be carried out using one or more methods from the methods **Seismic Coefficient** (**SCM**), **Equivalent Lateral Force** (**ELFM**), **Response Spectrum** (**RSM**) and **Modal-Time history** (**MTHM**) Methods. **SCM**, **ELFM** or **RSM** may produce response quantities with magnitudes bigger or smaller than those of refined method (**MTHM**). How big or small are the magnitudes in comparison with those of the refined method? In other words, are the magnitudes of **SCM**, **ELFM** or **RSM** overestimated or underestimated when contrasted with those of the refined method (**MTHM**)? Answering these questions through detail investigation is the core objective of this study.

In order to meet the core objective, an investigation of the seismic analysis methods of intake towers was conducted. The investigation was conducted by performing elastic seismic analysis of a squat free-standing intake tower, using the conventional and refined methods; and comparing the results of the analysis.

The investigation started by selecting a suitable intake tower and its location for the study. In this regard, the squat free standing intake tower in kesem Dam irrigation project, in Afar Regional State, was found to be suitable. The project is located in East African Rift Valley which is largely prone to earthquake excitations.

After selecting the intake tower and its location, the next step was structural, material and hydrodynamic modeling. Following the modeling, in put ground motions in form of response spectra and ground acceleration time-histories were developed. Next, seismic analysis of the intake tower was carried out using the models and the input ground motions; and applying each of the methods at a time. Finally, the results of the analysis were examined.

From the examination, the study concluded that the magnitude of response quantities computed with **SCM**, **ELFM** or **RSM** were significantly different from those of the refined method. Moreover, the study concluded that the magnitudes of the response quantities computed with three methods were underestimated. So, **SCM**, **ELFM** or **RSM**, especially **SCM**, are inappropriate for detail seismic analysis of squat free-standing intake towers.

As result, the study decided that **MTHM** shall be used for final and detail elastic seismic analysis of free-standing squat intake towers. However, further investigation are required in order to extend

the conclusion to other classes of intake tower such as free-standing slender intake towers and inclined intake towers. Similarly, other investigations are desirable in order to extend the conclusions of this study to inelastic analysis methods of intake tower.

LIST OF FIGUIRES

LIST OF TABLE

LIST OF NOTATOINS

a =ACCELELOGRAM.

ACC-1= A SET OF ARTEFICIAL GROUND ACCELERATOIN TIME HISTORIES, NUMBER-1.

ACC-2= A SET ARTEFICIAL GROUND ACCELERATOIN TIME HISTORY, NUMBER-2.

ACC-2= A SET ARTEFICIAL GROUND ACCELERATOIN TIME HISTORY NUMBER-3.

C_e =DIMENSOINLESS PRESSURE FACTOR.

$Coef_x$ =COEFFECIENT FOR STIFNESS CONSTANT IN THE DIRECTOIN OF X-AXIS.

$Coef_y$ = COEFFECIENT FOR STIFNESS CONSTANT IN THE DIRECTOIN OF Y-AXIS.

C_U= UNDRAINED SHAER STRENGTH OF FOUNDATOIN SOIL.

D=Strong motion duration for rock site.

E =MODULUS OF ELASTICITY OF CONCRETE.

ELFM =EQUIVELENT LATERAL FORCE METHOD.

EM=ENGINEERING MANUAL.

F_{xr} = LATERAL FORCE AT r^{th} NODE IN THE X-DIRECTOIN.

$F_{x\,n}$ =LATERAL FORCE ABOVE r^{th} NODE IN X-DIRECTOIN.

$F_{y\,n}$ = LATERAL FORCE ABOVE r^{th} NODE IN X-DIRECTOIN.

F_{yr} = LATERAL FORCE AT r^{th} NODE IN THE Y-DIRECTOIN.

g=ACCELRATOIN DUE TO GRAVITY.

I_{topX}=MOMENT OF INERTIA ABOUT X-AXIS FOR THE TOP MOST ELEMNT.

I_{topY}= MOMENT OF INERTIA ABOUT Y-AXIS FOR THE TOP MOST ELEMNT.

I_{baseX} = MOMENT OF INERTIA ABOUT X-AXIS FOR THE BOTTOM MOST ELEMNT.

I_{baseY} = MOMENT OF INERTIA ABOUT Y-AXIS FOR THE BOTTOM MOST ELEMNT.

K_x =STIFFNESS CONSTANT IN THE DIRECTOIN OF X-AXIS.

K_Y =STIFFNESS CONSTANT IN THE DIRECTOIN OF X-AXIS.

L = TOTAL HIEGHT OF INTAKE TOWER.

L_{x1} = MODAL EARTHQUAKE EXCITATOIN FACTOR ALONG X-AXIS.

L_{y1} = MODAL EARTHQUAKE EXCITATOIN FACTOR ALONG Y-AXIS.

m_x = THE SINGLE LUMPED MASS ALONG X-AXIS.

m_{xr} =TOTAL MASS LUMPED AT r^{th} NODE ALONG X-AXIS.

M_{xr} =THE BENDING MOMENT ABOUT X-X AT r^{th} NODE LEVEL.

M_{yr} = THE BENDING MOMENT ABOUT Y-Y AT r^{th} NODE LEVEL.

m_{yr} = TOTAL MASS LUMPED AT r^{th} NODE ALONG Y-AXIS.

m_y = THE SINGLE MASS ALONG Y-AXIS.

M_s =EARTHQUAKE MAGNITUDE.

MTHM=MODAL-TIME HISTORY METHOD.

MWL=MAXIMUM WATER LEVEL.

n^{th}=DESIGNATOIN NUMBER OF NODES OF BEAM-COLUMN MODEL.

p_{emh}=LOAD DUE TO INEERTIA.

P_{ewh}=RESULTANT HYDRODYNAMIC LOAD.

PF_{x1}=MODAL PARTICIPATOIN FACTOR IN X-DIRECTOIN

PF_{y1}= MODAL PARTICIPATOIN FACTOR IN Y-DIRECTOIN

r =IDENTIFICATOIN NUMBER FOR ALBTRARY NODE OF THE BEAM-COLUMN MODEL

S_{xA} = SPECTRAL ACCELERATOIN IN X-DIRECTOIN.

S_{yA} = SPECTRAL ACCELERATOIN IN y-DIRECTOIN.

SCM=Seismic Coefficient Method.

SRSS =SQUARE ROOT OF SUM OF SQUARES.

RSM=RESPONSE SPECTRUM METHOD.

t_o = INTIAL TIME OF GROUND ACCELERATOIN.

t_f = FINAL TIME OF GROUND ACCELERATOIN.

V_{xr} = THE TOTAL SHEARFORCE IN X-DIRECTOIN SUMPED UP AT r^{th} NODE.

V_{yr} = THE TOTAL SHEARFORCE IN Y-DIRECTOIN SUMPED UP AT r^{th} NODE.

V_s=VERSUS.

Z =WATER DEPTH MEASURED FROM ITS SURFACE

Z_{max} =MAXIMUM DEPTH OF WATER.

Φ_{r-1} = THE DEFLECTED SHAPE FUNCTOIN OF r^{th} NODE.

a_h = HORIZONTAL SEISMIC COEFFICIENT.

γ_w = UNIT WIEGHT OF WATER.

ω_{x1} = FREQUENCY OF EXCITATOIN IN THE X-DIRECTOIN

ω_{y1} =FREQUENCY OF EXCITATOIN IN THE Y-DIRECTOIN

ξ =DAMPING RATIO

1 INTRODUCTOIN

Usually, reinforced concrete intake towers located in earth quake prone regions require seismic analysis. The seismic analysis may be carried out with the methods such as **Equivalent lateral Force (ELFM)**, **Seismic Coefficient** (**SCM**) and **Response Spectrum** (**RSM**) or/and the more refined, **Modal-Time History** (**MTHM**)method(s).

The four methods mentioned here above, have special features peculiar to each as well as features common to all. For example, Equivalent lateral Force Method is unique in that it idealizes earth quake loads as static ones; however, the rest are devoted to representation of the earthquake loads as dynamic loads. Moreover, Response Spectrum Method, on its part, is unique such that it can be used to calculate maximum earthquake responses regardless of their time of occurrences. On the contrary, Unlike the Response-Spectrum Method, Time-History Method may be employed to calculate the maximum responses along with their time of occurrences.

These and other unique and common features, owned by the methods, may be the reasons why the methods often considered being different. Are they really different? If the answer is yes, then what is the extent of their difference? These are questions that this study going to answer after making quantitative and qualitative comparisons among response quantities computed with the respective methods.

Answering these questions requires detail and careful investigations. Accordingly, an investigation was carried out by conducting seismic analysis of an intake tower with two methods that represents the conventional methods and the more refined method (Modal-Time History Method) by applying each of them at a time.

The investigation started by selecting an intake tower from two broad categories of intake towers. The two broad categories of intake tower are inclined intake tower and free standing intake tower. The class of inclined intake towers includes intake towers that totally leaned against abutment for purpose of support, while the class of the free standing ones consists of intake towers that stand straight upward and primarily supported on foundation beneath it.

Free-standing intake towers may further be classified as slender or squat based on their geometric configurations. If an Intake towers has width to height ratio less than 1/10, then it is slender, otherwise it is squat.

Because most of in take towers constructed so far are from the free-standing class (**U.S Army of Corps of Engineers**, (**2003a**)), a squat intake tower from this class has been chosen for purpose of assessing the three methods.

The four methods will be employed, separately, to run the seismic analysis of the squat free standing intake tower. After the analysis, the results will be compared quantitatively as well as qualitatively to decide whether the conventional methods produce response quantities whose magnitudes are significantly different from those of the refined method.

Seismic Coefficient Method is still being used in Ethiopia for detail analysis of intake towers (**WWDSE et al**, **2010a**; **WWDSE et al**, **2010b**; and **WWDSE et al**, **2010c**).This method has been identified as being obsolete (**Novak et al** (**2007**)).So, the study has purpose of examine the extent of obsolescence of the method by comparing the magnitude of response quantities computed using the method with those of refined method, there by concluding appropriateness of the method for practical applications.

Therefore, generally, purpose of carrying out the investigation, in this study, was to establish the extent of magnitude difference among the respective response quantities computed with the four methods, thereby comparing the output of the conventional methods with the output of the refined method.

The desire for carrying out the investigation has been inspired by the need for having in-depth knowledge regarding the seismic analysis methods of intake tower. Prior to this study, there had been no literature which discussed in detail about the magnitude difference among the methods when applied for seismic analysis of intake tower.

2 LITRATURE REVIEW

Several studies have been conducted to examine the factors that affect seismic responses of intake towers. The factors often under investigations are the following: water-structure interaction, soil-structure interaction, and multiple support excitation effects.

The responses of intake towers to seismic excitation are affected by water-structure interactions; **Vidot et al**, (**2004b)** quoted **Daniel** and **Taylor** (**1975**) to state that the response of intake tower under dynamic loading can be strongly influenced by its interaction with reservoir water outside and inside it.

The influence may manifest it self by elongating natural period of intake tower which in turn changes the corresponding response spectrum ordinate ,as result altering seismic forces (**spyrakos** and **Chaojin Xu** (**1997**)) .

In addition, the study of **spyrakos** and **Chaojin Xu** (**1997**) revealed that there existed interaction between the reservoir's hydrodynamic load and flexible foundation soil beneath the intake tower. The Hydrodynamic load and the flexible soil foundation interact in such away that deflections, shear and moment of the intake tower are more than they are under rigid foundation assumption. **Spyrakos** and **Chaojin Xu** (**1997**) also investigated effects of intake tower configurations and water-structure interaction on soil-structure interaction. The investigation concluded that water-structure interaction negates the soil-structure interactions given the intake tower is squat; however, soil-structure interaction gets magnified by water-structure for slender tower.

Now days, after several researches, the belief that intake towers' seismic response are magnified by hydrodynamic load has become an established fact. Consequently, when evaluating the three seismic analysis methods of intake towers, the hydrodynamic effect on seismic response will be taken into consideration.

The water-structure interaction effects may be taken into consideration by converting hydrodynamic loads into equivalent masses (**U.S Army Corps of Engineers, 1999**).
The equivalent masses will be placed at nodes of models of intake tower as if they were added masses of the structure.

Soil-structure interaction is the other factor that significantly influences response of intake tower to seismic excitation (**Vidot et al**, **2004a**). Furthermore, **Vidot et al**, (**2004C)** citing **Goyal** and **Chopra** (**1989b**) commented that the interaction increases the fundamental period of intake towers and effective damping because of flexibility and energy dissipation of the soil foundation. The effect will be worse if the fundamental period of foundation soil is approximately equal to the fundamental period of intake tower. However, the fact that a structure has been constructed on soil foundation alone does not necessarily imply substantial soil structure interaction.

Soil-structure interaction is substantial at times when stiff intake towers, with large height to footing radius ratios, are founded on flexible soil strata **(Vidot et al**, **2004a)**.

One of the way of accounting for soil-structure interaction effect is by attaching springs and dash-pots to base of the structure or to different levels of non-homogenous soil strata under the structure, during seismic analysis of an intake tower , (**Dowrick, 1978**).In this way, the intake tower can be modeled as beam-column system. On their part, the springs and dash-pots may be placed at contact point between the model and foundation for homogenous soil stratum .on other hand, for non-homogenous soil strata, the springs and the dash-pots will be interconnected in series ,beneath the foundation.

Alternatively, Finite element modeling may be used to account for the soil-structure interaction. In this alternative approach, certain depth of soil foundation along with the superstructure will be idealized as a unit during seismic analysis of the intake tower (**U.S Army Corps of Engineers, 2007a**).

The other factor that possibly affects the seismic response of intake tower is the bridge–intake tower interaction .It is the factor that needs attention especially during modeling of an intake towers connected to access bridge. If the connected bridge is light, then the intake towers may be modeled as independent entity without the bridges. In the case of massive access bridge connection, the bridge and intake tower will be modeled as a single composite structure (**U.S Army Corps of Engineers**, (**2003b**)).

Once it is decided that modeling of the intake tower and the access bridge as a single composite structure is important, the next issue requiring similar decision would be regarding the design ground motions. Generally, in single composite models, intake tower

base level may be different from the bridge supports' levels, or piers' bases level; hence, the geology at the base of the intake tower may be different from the geology at the base of the bridge supports. The difference in geology may result in different ground accelerations during earth quake excitations. In situations like this, one may opt to use different input ground motions at intake tower and pier base levels so as to account for multiple support excitations.

Regarding effect of multiple support excitations on response of intake, a study has been conducted by U.S. Army Corps of Engineers (**Vidot et al**, **2004**).

The out come of the study implied that multiple support excitation effect on seismic response of composite bridge-intake tower system is negligible. Hence, defining identical design ground motions for all of the support of the composite model suffice.

Based on the conclusion of the study, for the composite bridge-intake tower system the multiple support excitation effect may be disregarded during defining the design ground motions.

3 SEISMIC RESPONSE ANALYSES OF AN INTAKE TOWER

In this study, the seismic responses analyses of an irregular intake tower have been conducted using **Seismic Coefficient**, **Equivalent Lateral Force**, **Response Spectrum**, and **Modal-Time History** analysis methods.

The seismic analyses were conducted based on two general approaches. In the first approach, initially, the seismic analysis of the intake tower was performed, as if it were regular.

later the effect of irregularity, torsional moment of the intake tower, was incorporated by multiplying the lateral inertia forces, for a given vertical portion of the intake tower, by their eccentricities from center of rigidity of the intake tower (**U.S Army Corps of Engineers, 2003b**).This approach was followed when conducting seismic analysis of the intake tower with Equivalent lateral force and Response Spectrum Methods for which the intake tower was discretize as beam-column system.

In the second approach, using software, the intake tower was modeled by three dimensional shell elements to take its irregularity into account directly. Since the software program automatically caters for the eccentricity effects, there is no need of worrying about the irregularity of the intake tower.

Following the modeling, the seismic analysis of the three dimensional model was performed using the Modal-Time history method.

Before conducting the seismic response analysis, determination of design ground motions, hydrodynamic loads have been carried out as preliminary steps.

In order to execute the preliminary steps, first suitable project and its intake tower have been be chosen in such a way that they provide input data good enough to generate big seismic response.

Data of the intake tower, which is chosen as suitable, will be used to derive inputs for its seismic analysis.

3.1 SELECTION OF SUITABLE PROJECT SITE AND AN INTAKE TOWER

Kesem Dam irrigation project site and its intake tower, in Afar Regional State, were selected as suitable site for conducting the study on the seismic analysis methods of intake towers.

The project and its intake tower were chosen for the study because of the expectation that the seismic response quantities of the intake tower would be significant. The response quantities would be significant since the project and its intake tower are located in a region of high seismicity.

The seismicity high is due to the fact that the project is expected to be exposed to earthquakes whose magnitude could be as high as **7.1,** on Richter scale (**Geophysical Observatory, 2005**). As result of the location of the project in high seismic region, the input ground motion will be so large as to cause sensible and comparable magnitudes of the response quantities.

Moreover, the seismic responses of an intake tower may be large provided that they are analyzed for maximum credible earthquake (**MCE**). **MCE** is the greatest design ground motion that a source of earth quakes can produce (**U.S Army of Corps of Engineers, 1995).**

MCE are usually specified for seismic analysis of critical intake towers as per recommendations of manual **ER 1110-2**-**1806**. The manual categorizes an intake tower as critical one when the intake tower is in a project with high seismic hazard potential rating. In addition, the manual rates seismic hazard potential of a project as being high when the failure of, at least, one of its component structure entails loses of life, demolition of properties destruction of the environment.

For that matter ,The Kesem dam and irrigation project seismic hazard potentials may be designated as being high since the seismic failure of the its main dam or intake tower, ensues lose of life ,demolition of properties and destruction of the environments.

3.2 GEOMERY OF THE INTAKE TOWER

Kesem intake tower is free-standing intake tower with total height of **41**m and with rectangular cross section with over all dimensions of **15.38m** by **12.03m**.Out of the total height only **27.45m** is effectively freestanding while rest is embedded in concrete backfill. The elevated view of the intake tower is portrayed by **FIGURE 3.1 while FIGURE 3.2 and 3.3 depict the actual horizontal cross-sections**.

At top of the intake tower, a control-room has been constructed to monitor the amount of water release through the intake tower. A foot bridge with 2.5m width and 95m length spans from the top of the main dam the control-room of rectangular cross-section.

The rectangular cross section has some openings positioned unsymmetrical. The unsymmetrical positioning of opening is largely responsible for in plan irregularity of the intake tower. In addition, added masses from the access bridge and crane did contribute to the in plan irregularity of the intake tower. They form the irregularity by causing the non – uniform mass distributions in plan.

Based on the actual cross-section, shear center location of the intake tower may be determined manually. However, the manual calculation of the shear centers based on this actual section was so involved because of irregularity of the actual cross-section; therefore, a modification was introduced to the actual section so as to create simple section for easy estimation of the shear center.

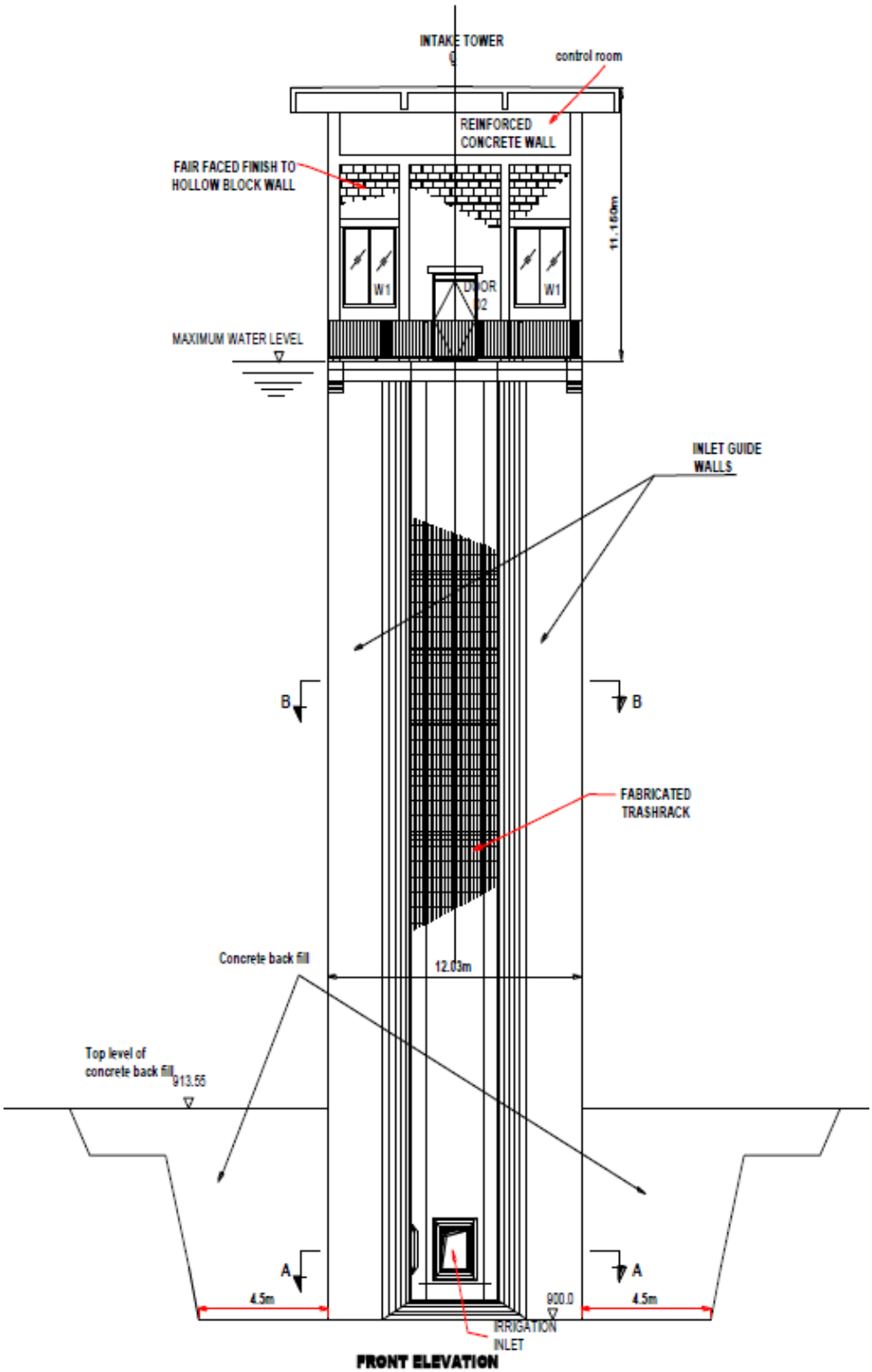

FIGURE 3.1 FRONT ELIVATOIN OF KESEM INTAKE TOWER

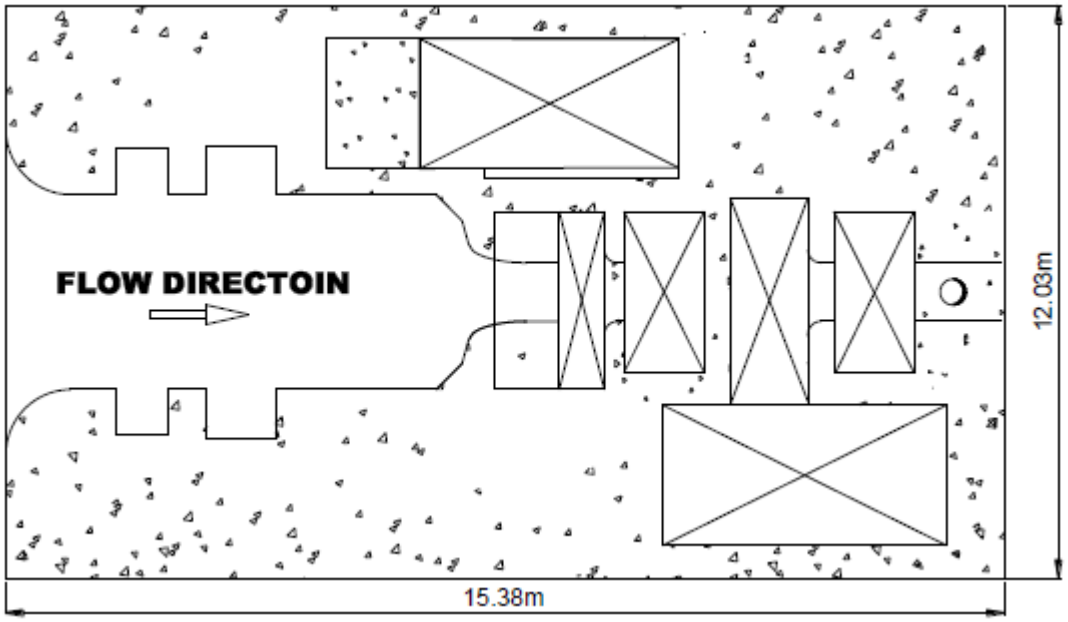

FIGURE 3.2 Horizontal SECTOIN B-B of KESEM INTAKE TOWER

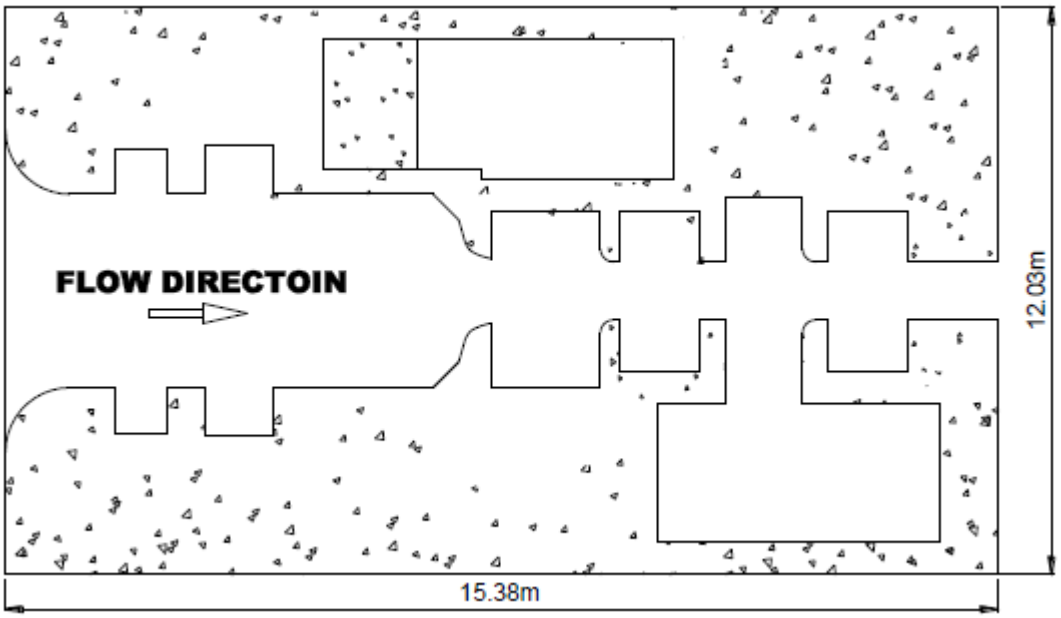

FIGURE 3.3 Horizontal SECTOIN A-A of KESEM INTAKE TOWER

The shear center of the simplified section (u-shaped simplified section) was determined assuming that the shear flow of the section is similar to that of thin section; the thin section has the configurations of the simplified section.
(**Farrar C.R.** and **Duffey T.A.** (**1995**)).

Moreover, the simplified section was accepted as basis for calculation of other section properties such as cross-sectional area and moment of inertia.

The section properties of the simplified section can be compared to that of the actual section using the numerical values listed in **TABLES 3.1**, **3.2** and **3.3**. The difference in numerical value of section properties of the two sections may be considered as insignificant.

In order to justify the claim that the difference in numerical value of section properties of the two sections can be considered as insignificant, seismic analysis of the intake tower were carried out based on beam column model. The results of the analysis (base shears and moments) are tabulated in **Appendix-G**.

After the analysis, the results of the analyses were examined. The examination showed that, at maximum, the base shear and moment magnitudes for the simplified section are **8.66%** and **6.89%** lower than the base shear and moment magnitudes for the actual section. This percentage of magnitude difference between the base shear and moment of the actual and simplified sections may be taken as tolerable. Consequently, the simplified section may serve to sufficiently idealize the section of the intake tower for seismic analysis.

The simplified section was assumed to remain uncracked during the seismic analysis of the intake tower despite level of stresses in the section (**U.S Army Corps of Engineers, 2007a**). Therefore, the stiffness of the intake tower was calculated based on the gross cross-section of the intake tower (**Mosley et al** (**2007**)).

The intake tower was classified as squat based on the height to width ratio of the intake tower. The width to height ratio of the intake tower was found approximately to be **0.44** which was bigger than **1/10** ratio; as result, the intake tower was classified as squat. The

width to height ratio was calculated taking the effective height of the intake tower as actual height.

The simplified section properties represented properties of sections of all beam elements along the height of Beam-Column model except the top most elements**.**

The top most element section properties were estimated considering lumped masses from the bridge, crane and control room in addition to the mass of the intake tower. As the result, the mass centers and the associated eccentricities of the top most element differed from those of the other elements.

The section properties of the actual section, the top most element and elements other than the top element are listed in **TABLES 3.1**, **3.2** and **3.3** respectively.

The differences in properties of the two simplified sections listed in **TABLE 3.2** and **3.3** lie only in mass centers and the related eccentricities. The difference is attributed to the fact that the section of top element includes the masses of the foot bridge, control room and the crane. Theses additional lumped mass altered the mass center of the section and consequently the eccentricities.

Cross sectional properties	Unit	Numerical values	
		X-axis	Y-axis
Sectional Area	m^2	91.3326	91.3326
Moment of inertia	m^4	1477.0578	1521.094
Shear area	m^2	51.88	66.065
Center of mass	m	-0.559	-2.438

TABLE 3.1 PROPERTIES OF THE ACTUAL SECTOIN OF THE INTAKE TOWER

Cross sectional properties	Unit	Numerical values	
		X-axis	Y-axis
Sectional Area	m^2	117.1826	117.1826
Moment of inertia	m^4	1576.5242	1735.03
Shear area	m^2	87.89	80.93
Center of mass	m	0	-2.3562
Center of rigidity	m	0	-8.81
Eccentricity	m	0	6.45
Product of inertia	m^4	0.00	

TABLE 3.2 SECTOIN PROPERTIES OF ALL BEAM ELEMENTS OTHER THAN THE TOP MOST ELEMENTS

Cross sectional properties	Unit	Numerical values	
		X-axis	Y-axis
Sectional Area	m^2	117.1826	117.1826
Moment of inertia	m^4	1576.5242	1735.03
Shear area	m^2	87.89	80.93
Center of mass	m	-0.147	-1.60
Center of rigidity	m	0	-8.81
Eccentricity	m	0.147	7.21
Product of inertia	m^4	0.00	

TABLE 3.3 SECTOIN PROPERTIES OF TOP MOST BEAM ELEMENT

The mass centers have importance in classifying intake towers as regular or irregular in plan. As per the engineering manual **EM 1110-2-2400** recommendation, an intake tower will be taken to be symmetrical provided that the center of gravity and the center of shear

are within 10 percent of the tower width when measured perpendicular to the direction of earthquake motion (**U.S. Army of Corps of Engineers**, **2003b**). In other words, the maximum tolerable eccentricity of the intake tower under consideration will be **10** percent of **12.03m** (±**1.203m**) and **10** percent of **15.38m** (±**1.503m**) along X and Y-directions respectively.

The expected eccentricity are calculated and entered in **TABLE 3.2** and **TABLE 3.2**.They are **0.0m** in X-direction and **7.21m** in Y-direction for the section of top most element. This section, therefore, can be considered as irregular as per the recommendation of the engineering manual.

For sections of beam elements other than the top most element, the eccentricity in X-direction is within the tolerable limit, **0.0m**<**1.23m**; however, the eccentricity in Y-direction is greater than the corresponding limit, **6.45m**>**1.503m**. So, these sections can be regarded as irregular too.

Over all, based on the examination of the geometry of the simplified section of the intake tower, the Beam-Column Model may be considered to be irregular in plan.

3.3 MAXIMUM RESERVOIR LEVEL OF THE PROJECT

Hydrological studies of the project have fixed the maximum top elevation of the reservoir of the project at **941m** above sea level. This maximum level is assumed to be level of reservoir during the excitation of design earthquake.

For purpose of estimating the hydrodynamic loads due to the design earthquake, hydro dynamically active depth of reservoir water was measured starting from top level of the concrete back fill (**913.55m**) up to the maximum reservoir level. Thus the difference between the two levels gave the hydro dynamically active depth of the reservoir to be **27.45m**.

3.4 SEISMIC HAZARD ANALYSIS OF THE PROJECT

A Chinese firm known by the name Mid-South Design and Research Institute carried out revised design of main dam for the Kesem Dam Irrigation project and released design report of the main dam in **2008**. The report stated that magnitude of peak ground acceleration of the maximum credible earth quake (**MCE**) of the project site was **0.3g** and the same magnitude of **MCE** was used for the revised design of the main dam (**Mid-south Design and Research Institute**, **2008**).Therefore, the magnitude of the **MCE** was endorsed, in this study, as magnitude of peak ground acceleration for seismic analysis of the intake tower.

Direction of the peak ground acceleration was assumed to be horizontal since nothing has been mentioned in the report concerning the direction of peak ground acceleratoin. Furthermore, the peak ground acceleration assumed to be the base rock acceleration; as result, the subsurface soil properties were taken into account when determining the surface ground motion at the base of the intake tower.

Moreover, because the report did not specify the magnitude of the peak ground acceleration in vertical direction, the magnitude of the peak vertical ground acceleration was estimated to be **0.27g by** multiplying the peak horizontal ground acceleration with factor of **0.9**.The factor was recommended by the **European code 8** to be adopt when a need a rise to know the vertical component of ground motion from the horizontal components of the ground motion (**Eucode-8**, **2003**).

The peak ground accelerations in turn were used to derive Horizontal Seismic coefficient. The coefficients were determined following recommendations stated in **U.S Army Corps of Engineer** manual number **EM-1110-2-6053**.It prescribes that the coefficient shall be two third of the horizontal peak ground acceleration. Thus, for 0.3g Peak Ground Acceleration, the Horizontal Seismic coefficient calculated to be **0.2**.

As per the seismic performance and serviceability recommendations released by **U.S. Army of Corps of Engineers** in its manual numbered **ER 1110-2-1806**, design earth quake for seismic analysis of the intake tower was required to be **MCE** (**U.S Army of Corps of Engineers**, **1995**).

The manual requires that a critical hydraulic structure in high seismic hazard situation shall be subjected to **MCE** for seismic analysis purpose. Since the intake tower was critical structure and based on the recommendation; **0.3g** and **0.27g**, maximum credible earthquakes, were accepted as design peak ground acceleration in horizontal and vertical direction respectively.

These maximum credible earthquakes were used to generate design ground motions in the form of elastic response spectrum; Later, the elastic response spectrum were used to develop design ground acceleration time histories.

Thus, the main dam revised design report in conjunction with the performance and serviceability requirements, set by the manuals, were used as bases for developing the design ground motions in the form of elastic specific response spectrums and ground acceleration time histories.

It is the site specific seismic hazard analysis that gave the **0.3g** peak ground acceleration. However, Ethiopian Building standard code specifies peak ground acceleration magnitude of **0.1g** for the region in which the intake tower is located (**EBCS-8**, **1995**).This magnitude of peak ground acceleration, **0.1g**, is found to be smaller than the magnitude obtained from site specific seismic hazard analysis, **0.3g**. The difference between the two magnitudes of peak ground accelerations (**0.1g** and **0.3g**) shows that Ethiopian building code standard may prescribe peak ground accelerations with magnitudes less than those of site specific seismic hazard analysis.

Therefore, for seismic analysis of massive structures or for seismic analysis of structures with greater importance, magnitudes of peak ground acceleration shall be determined based on site specific seismic hazard analysis instead of adopting them for the Ethiopian Building Standard Code,**EBCS-8**.

3.5 DEVELOPMENT OF ELASTIC RESPONSE SPECTRA

In compliance with the guidelines of the manual **ER 1110-2-1806**, elastic response spectra were developed so as to be utilized as inputs for seismic analysis of the intake tower (**U.S Army Corps of Engineers**, **1995**).

The elastic response spectra were developed through two steps; first shapes of response spectra were selected from provisions of **Eurocode**-**8**; second the shapes were multiplied with the peak design ground accelerations to obtain the elastic response spectra in horizontal as well as vertical in direction (**Noh et al.** (**1999**)).

The Euro-code provisions were applied because they stipulate separate relations for the determination of the shapes of the horizontal and vertical response spectra. By applying these relations, horizontal and vertical response spectra, with different shapes, were obtained.

The determination of the shapes depends on the undrained shear strength ($\mathbf{C_U}$), Standard Penetration Test blow counts, or average shear wave velocity of foundation beneath a structure for which the response spectra would be developed.

In addition to the site soil properties, for this study, shapes of responses spectra were selected depending on the following parameters: damping ratio of the concrete material (**ξ**), and the earthquake magnitude ($\mathbf{M_S}$) (**Eurocod-8**, **2003**).

The effect of subsurface soil conditions on shapes of response spectra have been catered for, through incorporation of the site soil parameter, the undrained shear strength ($\mathbf{C_U}$).
The values of the parameters with which the shapes of response spectra have been determine are given below:

1) $\mathbf{C_U=40KN/m^2}$ (**WWSDE and WAPCOS** (**2005**))
2) **ξ =5 %** (**U.S Army Corps of Engineers, 1999**)
3) $\mathbf{M_s=7.1}$ (**Geophysical Observatory, 2005**)

Using the provision of the code, two shapes were determination for three simultaneous design ground motions occurring in each of three perpendicular directions.

The three simultaneous ground motions are: two identical, orthogonal, horizontal response spectra, and a vertical response spectrum. The horizontal site response spectra and vertical spectrum have been developed taking into and assuming simultaneous occurrence of earth quake.

Therefore, the response spectra represent surface ground motions in three mutually perpendiculars directions which were applied directly at base of intake tower models, as an input for seismic analysis of the intake tower using **RSM** and **ELFM**.
The response spectrums are depicted by the following two figures, **FIGURE 3.4** and **3.5**.

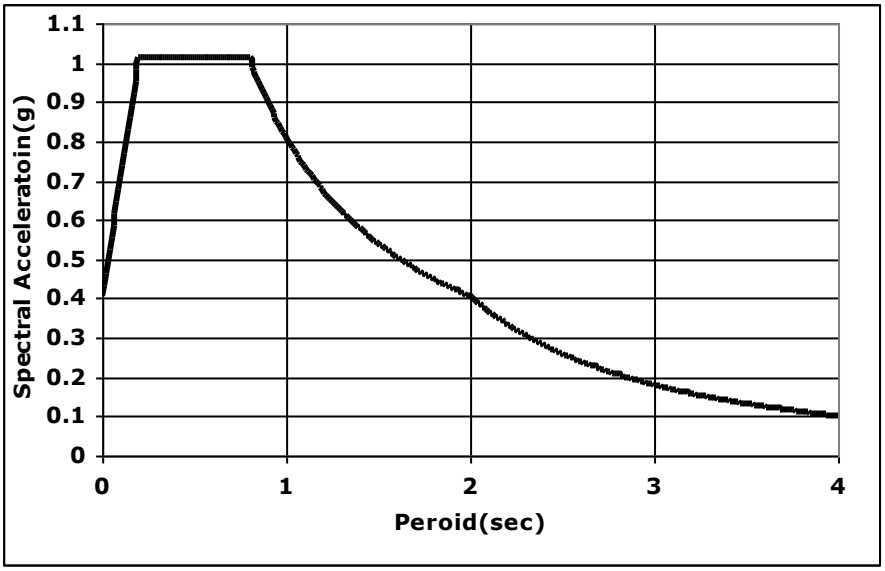

FIGURE 3.4 HORIZONTAL DESIGN RESPONSE SPECTRUMS

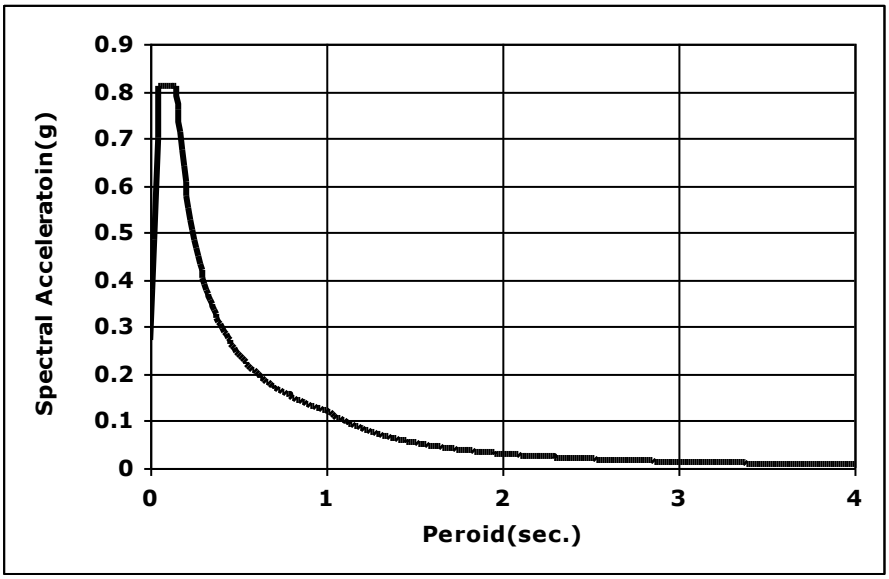

FIGURE 3.5 VERTICAL DESIGN RESPONSE SPECTRUM

Furthermore, the response spectra were used as target response spectra in order to generate artificial acceleration time histories for seismic analysis of the intake tower with **MTHM**.

3.5.1 CRITICAL INCEDENCE DIRECTOINS OF THE DESIGN GROUND MOTOINS

As per the quotations of **U.S. Army of Corps of Engineers** (**2007b**), **Wilson and Button** (**1982**)**, Smedy and Der Kiureghian** (**1985**); **Lopes and Torres** (**1997**) studied the effects of earthquake direction of incidence on response of structures.

After analyzing the studies, **U.S. Army of Corps of Engineers** (**2007b**) concluded that for the special case of identical spectra along the two horizontal directions, the structural response does not vary with the angle of incidence, i.e. any direction is a critical direction.

So, for this study, the critical directions of incidence of the horizontal design earth quake were taken to be parallel to the global X and Y-directions for the seismic analysis of intake tower with the three methods. These global directions were identical to the global direction of the simplified intake tower section.

3.6 DEVELOPMENT OF ARTEFICIAL GROUND ACCELERATOIN TIME-HISTORIES

U.S. Army of Corps of Engineers (2003a) recommended that at least three recorded or artificially generated acceleration time-histories for each component of the ground motions in three directions shall be utilized as input to carry out seismic analysis of hydraulic structures with Modal Time-History analysis method.

Moreover, according to the recommendation, the artificial or the recorded ground acceleration time-histories shall have response spectra that fit the target response spectra.

Accordingly, three sets of artificial ground acceleration were generated using software known by the name SIMQKE. Each set consists of three artificial accelerograms. In each set, two of the artificial accelerogram were developed to simulate the two mutually perpendicular horizontal ground motions while one of them was generated to simulate the vertical ground motion. The first set of accelerogram was designated as ACC-1 and the remaining two sets were designated as ACC-2 and ACC-3. Some of the artificial accelerograms are shown below along with their designations in FIGURES 3.6, 3.7, 3.8,and 3.9.
Generation of the artificial ground accelerations was preferred to obtaining of actually recorded ones due to lacking of sufficient and strong motion data of the latter.
However, with the software SIMQKE, it was possible to simulate all of the artificial accelerograms in such a way that their response spectra were compatible with the target response spectra. The response spectra of one of the horizontal and the vertical components of ACC-1 are depicted in FIGURES 3.10and 3.11 respectively.

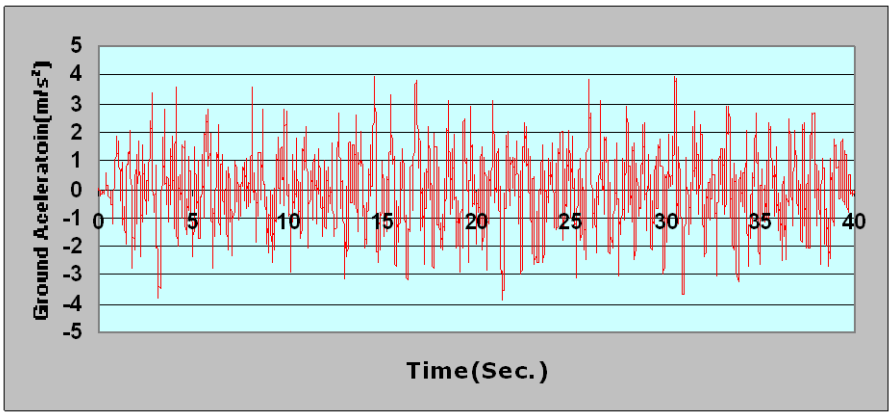

FIGURE 3.6 TIME-HOSTRY OF ONE OF THE HORIZINTAL COMPONENT OF ACC-1

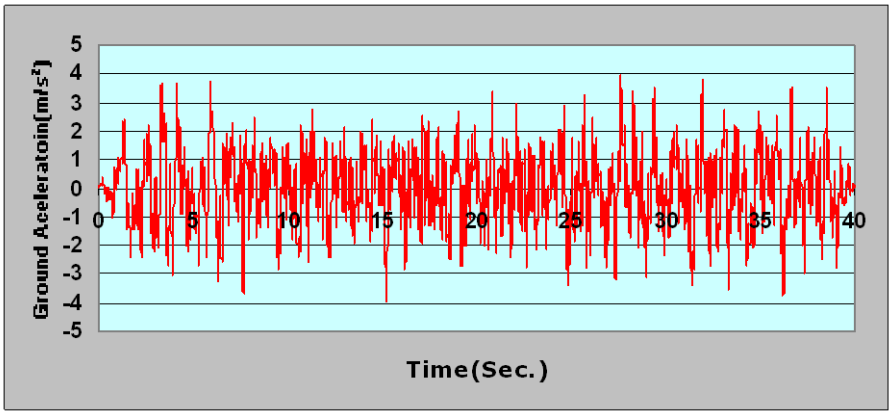

FIGURE 3.7 TIME-HOSTRY OF ONE OF THE HORIZINTAL COMPONENT OF ACC-2

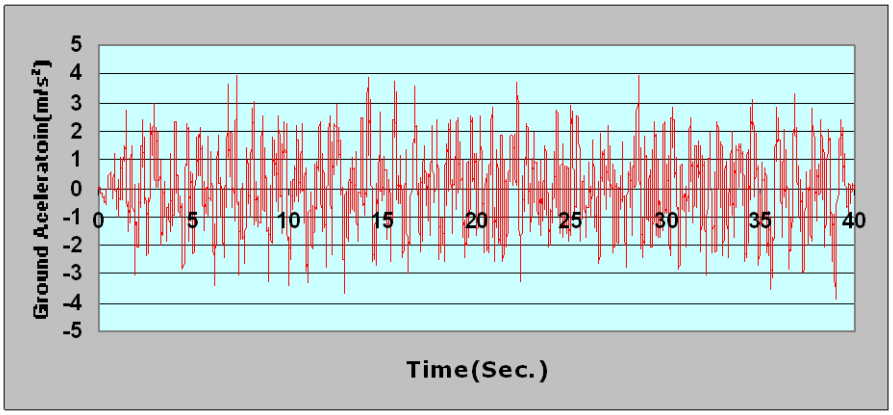

FIGURE 3.8 TIME-HOSTRY OF ONE OF THE HORIZINTAL COMPONENT OF ACC-3

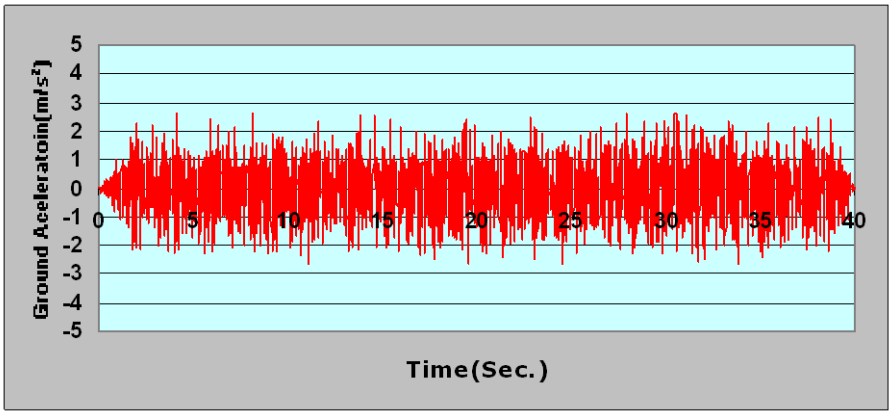

FIGURE 3.9 TIME-HOSTRY OF ONE OF THE VERTICAL COMPONENT OF ACC-1

In addition to the conformity of response spectra of the accelerations to that of the target response spectra, the accelerations are expected, as per the **U.S. Army of Corps of Engineers (2003a)**, to have strong motion duration comparable to duration of the target responses spectra. Moreover, it stipulates that the strong motion duration of artificial acceleration time histories be within a factor of **1.5** of the design strong motion duration.

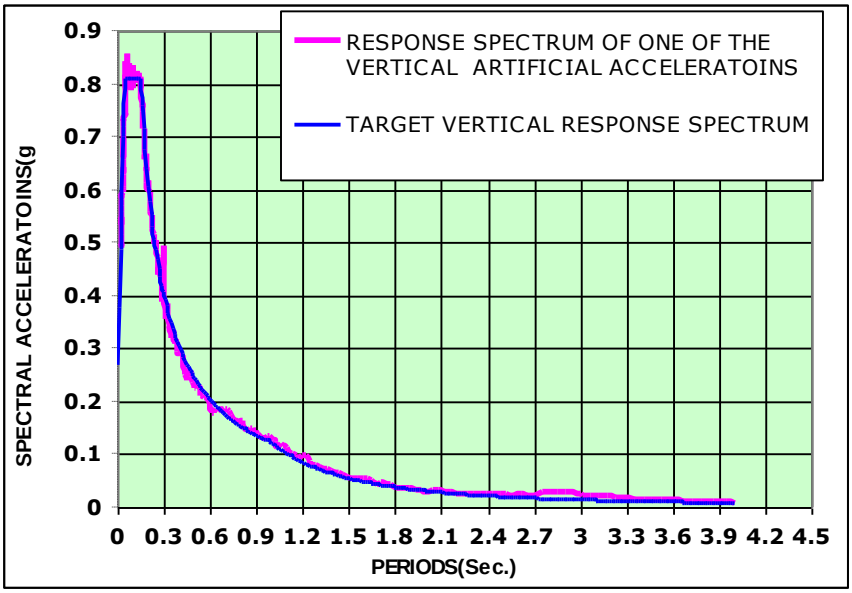

FIGURE 3.10 VERTICAL TARGET SPECTRUM V_s SPECTRUM OF ONE OF THE VERTICAL AERTEFICIAL ACCELERATOINS

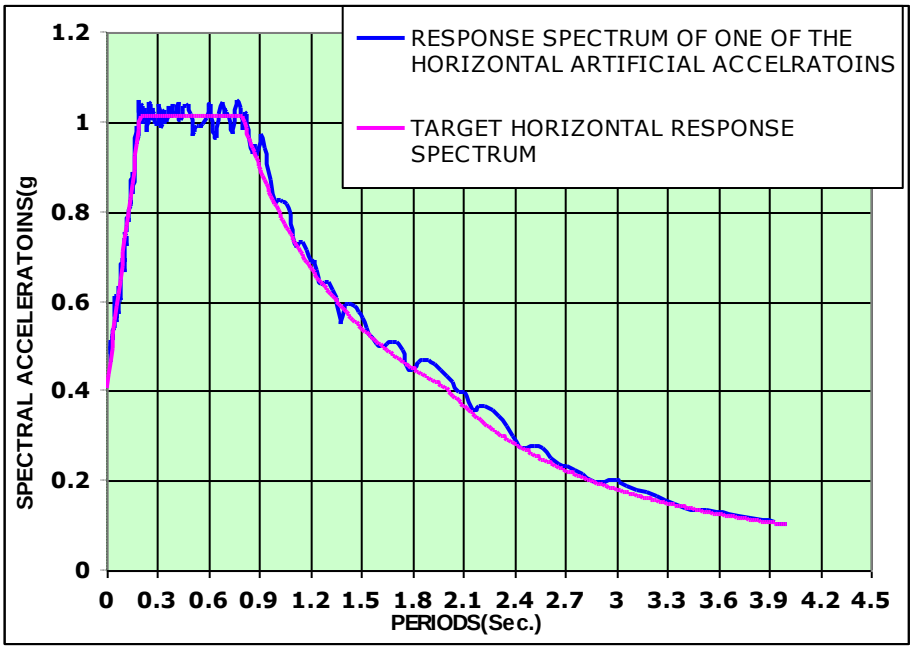

FIGURE 3.11 HORIZONTAL TARGET SPECTRUM V_s SPECTRUMOF ONE OF THE HORIZONTAL AERTEFICIAL ACCELERATOINS

The strong motion durations of the accelerations were calculated using a correlation developed by **Husid plot** (**U.S. Army Corps of Engineers,** (**2003a**)). The Correlation, which is given below here, used to calculate cumulative energy build up of the

accelerograms with time. Using the correlation, strong motion duration is defined as the time take for the commutative energy to build up from 5% up to 95%.

$\int_{t_o}^{t_f} a^2 dt$ where,

a = accelerogram,

t_o = initial time of ground accelerations and,

t_f = final time of ground accelerations.

The correlation has been employed to estimate the energy of the artificial accelerograms as well as their strong motion durations. For instance,the strong motion duration of one of ACC-1 was estimated and found to be **34.78** seconds, as shown in **Figure 3.12**. In similar fashion, the strong motion duration of the rest artificial accelerograms were computed and found to be in the vicinity of **34.78** seconds.

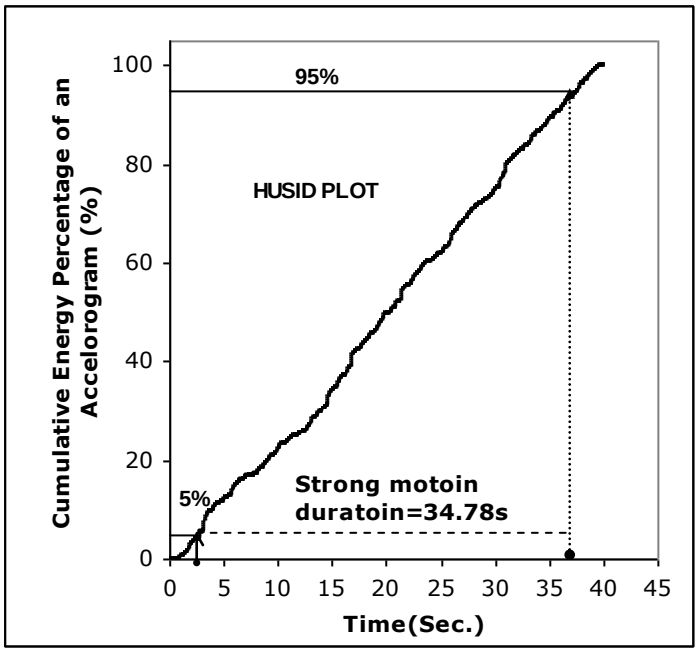

FIGURE 3.12 HUSID PLOT OF ON OF THE COMPONENTS OF ACC-1

Similarly, the design strong motion duration was estimated based on the empirical relation given in the engineering manual **EM 1110-2-6051** for rock site by **U.S. Army of Corps of Engineers (2003a)**. As per the manual, for soil site, the value of strong motion duration obtained using the relation will be multiplied by factor between 1.5 and 2. The Empirical relation is shown here below.

$D = 10^{(0.423M_s - 1.83)}$ Where,

D=Strong motion duration for rock site (in seconds), and

M_s=Earthquake Magnitude (in Rehctor scales).

The design strong motion duration for the target responses spectra was calculated using the above relation and the result was multiplied by factor of two in order to account for effect of the soil in the site .As result, the design strong motion duration was found to be **34.5** seconds.

Therefore, the strong motion durations of the artificial accelerations were satisfactory since they were multiple of the design strong motion by factors less than **1.5**.

3.7 MODELING FOR THE SELECTED INTAKE TOWER

In process of material modeling, numerical values of concrete material properties were obtained and defined as input to the computer program in preprocessing stage of finite element dynamic analysis of the intake tower. In addition to being inputs for computer programming analysis, the numerical value served also as inputs for seismic analysis methods that involve manual calculation.

Next to the martial modeling, structural object modeling of the intake tower, and hydrodynamic modeling were carried out to be used as inputs for seismic analysis of the intake tower.

3.7.1 MATERIAL MODELING

U.S. Army of Corps of Engineers (**2007c**) quoted **Bruhwieler (1990**) and said that in the absences of dynamic tests the dynamic properties of concrete can be extrapolated from the corresponding static property by multiplying them with certain recommended factors.

The recommended factors were used to multiply static concrete properties so as to get their corresponding dynamic properties. **TABLE 3.4** lists the dynamic properties of the concrete, obtained from the static material properties of the concrete through the multiplication.

Initially, the static martial properties of the concrete were obtained from, design standards, engineering manuals, and design document of the intake tower.

No	Parameters	Unit	Numerical values			Source for static value
			Static	Factor	Dynamic	
1	Mass per Unit Volume	Kg/m^3	2.5	1	2.5	(**EBCS-1**,**1995**)
2	Weight per Unit Volume	KN/m^3	25	1	25	(**EBCS-1**,**1995**))
3	Modulus of Elasticity	GPa	32	1.15	36.8	**(EBCS-2,1995)**
4	Cylindrical Compressive strength	Mpa	25	1.15	28.75	**From design drawing**
5	Poisson's Ratio	-	0.2	0.7	0.14	**(EBCS-2**,**1995)**
6	Damping Ratio	-	-	-	0.05	**EM 1110-2-6050**

TABLE 3.4 DYNAMIC MATRIAL PROPERTIES USED FOR THE ANALYSIS

In addition to the dynamic properties driven from static properties, the other dynamic property defined for seismic analysis of the intake tower was the damping ratio. The value of the damping ratio was defined to be **0.05** in accordance with the recommendation of the **U.S. Army of Corps of Engineers** (**1999**).

3.7.2 DETERMINATOIN OF HYDRODYNAMIC LOADS

The Goyal and Chopra's simplified added mass approach was employed to idealize the hydrodynamic loads acting on Beam-Column model as the equivalent added masses. After idealizing the hydrodynamic loads as equivalent added masses, they were lumped at the nodes of the Beam-Column model (**U.S. Army of Corps of Engineers**, **1999**).

Prior to the idealization of hydrodynamic load as the equivalent added mass, the sufficient number of nodes at which they would be lumped was determined. The purpose of the determination had been to accurately represent the distribution mass system of the intake tower as its equivalent lumped mass system. The node points of the Beam-Column Model were determined as part of structural object modeling in attempt to represent the distributed mass of the intake tower as equivalent lumped mass system.

For seismic analysis that involves the Beam-Column Model, the equivalent added masses were separately determined for hydrodynamic loads along two horizontal orthogonal directions, X-axis and Y-axis. For both axes, the estimation of the equivalent added masses are given in **APPENDIX-A**.

In the Appendix, **TABLE-A** shows that the hydrodynamic added masses of each of the two axes are not equal, because the hydrodynamic added mass depends on the dimension of intake tower perpendicular to the direction of the ground motion: since the intake tower is rectangular, the added masses along the two axes had different values.

Similarly, the same approach was employed too to idealize the hydrodynamic on Three Dimensional Models as equivalent added masses (**Johnson et al.** (**1993**)).The added masses were too lumped at the nodes of the Three Dimensional Model existing at the same level as the corresponding nodes of the Beam-Column model.

In the case of The Three Dimensional Model, the node points were determined in the attempt to sufficiently discretize the intake tower through mesh refining.

For Three Dimensional Model, the hydrodynamic added masses calculated for the Beam-Column Model at the levels of the nodes were adopted. Along each direction, the adopted hydrodynamic added masses were equally divided among the node of the Three Dimensional Model.

3.7.3 STRUCTURAL OBJECT MODELING

Generally two techniques were employed to idealize the intake tower for seismic analysis.
The first is rigid body modeling technique in which the intake tower was modeled as a single rigid body with integrity. The second technique is standard finite method with which the intake tower was idealized as though it was made up of number of interconnected elements.
The interconnected elements were of two kinds. The first kind consists of beam elements while the second comprises of predominant shell elements.

Using the two kind of elements two types of models were prepared. The first model type of models was beam-column or stick model, which was deemed by Army of corps of engineers as being appropriate for modeling of intake tower for seismic analysis using equivalent lateral force method (**U.S Army Corps of Engineers**, **2003**).

The second type of model, Three Dimensional Model, was made mainly out of shell elements. In addition to shell elements, it consists of beam and link elements.

Three Dimensional Modeling is proper for modeling of intake towers with appreciable irregularity (**U.S Army Corps of Engineers**, **2007**).

A finite element analysis software program has been employed to accomplish the process of representing the intake tower as beam-column and as three dimensional shell element models.

In order to understand the behaviors of the shell elements under external load, to evaluate the efficiency of the software in relation with shell element modes, and to build up operation know how of the soft regarding shell element analysis, a pilot study was conducted (**Cook**, **1995**).

The pilot study consisted of preparing, using the software, a simple shell element model whose configuration is similar to that of the three dimensional model of the intake tower.

After the preparation of the simple shell model, external loads were applied at suitable points on the model so that the reaction of the model to the external load can readily and manually be calculated.

Next, the reactions of the simple model to the external loads were analyzed with the software, and were calculated manually too.

Finally the results of the software analysis and manual calculation were compared. The comparison showed that:-

- The software is efficient in calculating section forces of shell element models.
- The shell elements of the software are suitable for three dimensional modeling of the intake tower.

3.7.3.1 THE RIGID BODY MODEL

Rigid body modeling technique may be used to represent structures with huge stiffness, for seismic analysis purpose. For instance, massive concrete structures to be constructed on flexible foundation may be idealized as rigid body. In addition, rigid body modeling

technique may be employed to model structures for static as well as dynamic stability analysis.

For this study, the intake tower was idealized with rigid body model for seismic analysis that applies Seismic Coefficient Method. The rigid body model is depicted in **FIGURE 3.13** below.

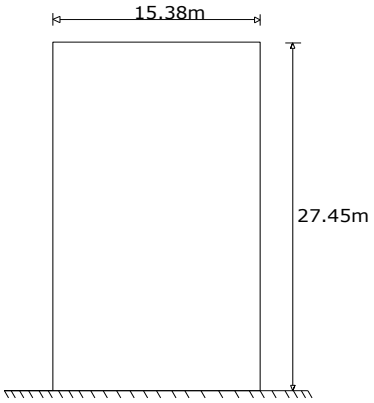

FIGURE 3.13 RIGD BODY MODEL OF KESEM INTAKE TOWER

3.7.3.2 BEAM-COLUMN MODEL

In this study, the finite element modeling of the intake tower as the Beam-Column Model was conducted in order to idealize distributed mass system of the intake tower like lumped mass system. The Beam-Column Model, the lumped mass system, was used to represent the intake tower in seismic analysis that involves Equivalent lateral Force and Response Spectrum Methods. The Beam-Column Model was portrayed in **FIGURE 3.14**.

The finite element modeling approach, among the others, was chosen because it is one of the best way of idealize distributed mass systems as lumped mass systems (**chopra, 1995**).

The finite element approach was used to discretize the intake tower with series of beam elements inter-connected at nodes. At the nodes, only two degree of freedoms was made available .The two degree of freedoms was transitional degree of freedom along X and Y axes.

A third degree of freedom in the Z-axis, vertical degree of freedom, is usually ignored during seismic analysis of intake tower idealized with beam column model.

The vertical degree of freedom is neglected because intake towers usually possess overwhelming stiffness in that direction, according to some authorities in the field of seismic analysis of intake tower (**Johnson et al.** (**1993**), **U.S Army Corps of Engineers**, (**2007**); and **Vidot et al**, (**2004**)).
The nodes of the intake tower served as point at which the distributed mass of the intake tower, hydrodynamic added masses, and masses of crane and bridge were all lumped. Because of the lumping of all the masses of the intake tower at the node, the beam elements between the nodes were idealized as massless.

The number of these nodes should be sufficient in order to appropriately idealize the distributed mass of the intake tower as lumped mass system. **U.S Army of Corps of Engineers** advises the use a minimum of five nodes to represent the distributed mass equivalent lumped mass. Therefore, to determine the sufficient number of nodes or beam elements, successive trial analyses were run with the Beam-Column Model by revising the mode number each time. As initially step, the trial began by selecting the number of the node to be four. The initial guess of number of sufficient nodes was selected deliberately to be four in order to it just below the recommended number, five.

In each trial, the number of nodes was chosen to be greater than the previous trials and the new beam-column model was analyzed with response spectrum method to determine base shear and base moment along and about X-Axis. The number of the node was kept on increasing in the succeeding trials until the difference in magnitude of the base shear and moments between the two last trials appeared to be negligible (**Cook**, **1995**). The trial analyses were performed revising the number of nodes each time and noting the difference in magnitude of base shear and moment at base of the Beam-Column Model.

The difference in magnitude of the base shear was regarded as negligible when the percent of the discrepancy between the base shears reached **0.103 %** at fourth trial. Similarly, the difference in magnitude of the moment at the base was taken to be insignificant when the discrepancy reached **0.203%** at fourth trial too.

The fourth trial was conclusive for the seismic analysis in X-axis and Y-axis in which the revised number of node the Beam-Column Model reached ten since the difference in magnitudes of the base shears and bending moments become inconsiderable.

Therefore ten was taken as number at which the intake tower could be sufficiently discretized for Equivalent lateral and Response Spectrum Methods of seismic analysis.

TABLES 3.5 and **3.6** depict the order of trials and the corresponding number of nodes; moreover, they described the percentage of difference between base shears of successive trials.

On its part, **FIGURE 3.13** shows the number of nodes of the final Beam-Column Model accepted after the successive trials. The Figure also shows numbers used to identify nodes of the model for defining inputs for seismic analysis and reporting the analysis results.

Trial No	Number of Beam Elements	Base Shear along X-Axis (KN)	Difference (%)
1	3	144438.69	-
2	5	143102.14	0.934
3	7	142830.06	0.19
4	9	142679.5	0.106

TABLE 3.5 DETERMINATOIN OF THE SUFFICIENT NODE NUMBER FOR SEISMIC ANALYSI ALONG X-AXIS

Trial No	Number of Beam elements	Base Moment about X-Axis (KN-m)	Difference (%)
1	3	3064150.9	-
2	5	2871842.8	5.91
3	7	2845225.2	0.936
4	9	2839456.3	0.203

TABLE 3.6 DETERMINATOIN OF THE SUFFICIENT NODE NUMBER FOR SEISMIC ANALYSI ALONG Y-AXIS

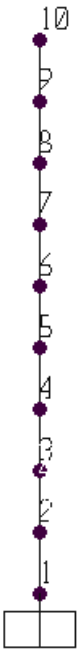

FIGURE 3.14 BEAM-COLUMN MODEL OF INTAKE TOWER

During the trial and error processes, masses of the intake tower, crane and bridge was lumped at tenth node of final beam column model along X-axis and Y-axis. Similarly, masses of the intake tower were lumped at the nodes from 1 up to 9 in the direction of both X-Axis and Y-Axis. The magnitudes of the added masses discuss here above are presented in **Appendix-B**.

Moreover, in each trial for determination of the sufficient number of nodes, the lumped masses of the intake tower and hydrodynamic added masses were recalculated as size of the elements change. The Change in sizes of the element altered hydrodynamic added masses and intake tower masses between the nodes of the each element of the Beam-Column Model. **TABLE–B** in **Appendix-B** lists the revised added mass at each trail.

3.7.3.3 THREE DIMENSOINAL MODEL

Three dimensional model was required to idealize three dimensional finite element model of the intake tower since it is consistent with Modal Time-History Method of seismic analysis.

The three dimensional modeling of the intake tower was carried out with help of beam elements, link elements, and shell elements.

The beam elements were used to idealize struts constructed between two 1.33m thick walls extruding out ward from left and right sides of 8.14m thick wall. The link elements, however, were introduced to introduce joint offset between center lines of shell elements representing the 1.33m thick walls and 8.14m walls. The 1.33m thick walls and 8.14m thick wall are depicted on **FIGURE 3.14** below

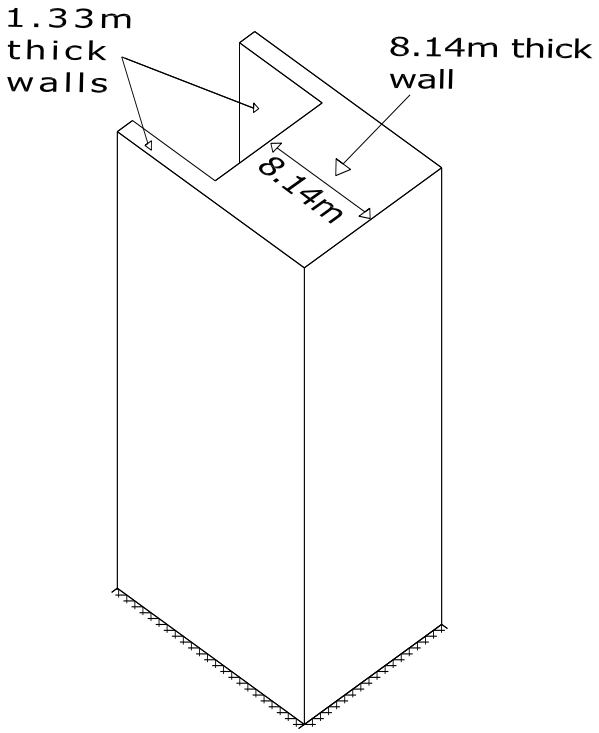

FIGURE 3.14 WALLS OF 3-D MODEL WITH 1.33m AND 8.14m THICKNESSES

1.33m and 8.14m walls were represented by shell elements with thickness of 1.33m and 8.14m respectively.

The dimensions of the rectangular cross-section of the intake tower exceeded one tenth of the effective height of the intake take tower.

That means, the effects of transverse shear deformations on vibration frequency and section forces are important **(U.S Army Corps of Engineers, 1999)**.Hence, the shell elements were prepared in such away that the effect of shear deformation on responses of the intake tower are included during the seismic analysis.

So as to include the effects of transverse shear deformations, all shell elements' dimensions were proportioned, during modeling and in each mesh refining process, keeping their thickness to span ratio greater than one over ten.

If the thickness to span ratio of shell elements exceed one over ten, then they are considered to be thick plates shell elements. Thick plates shell elements are formulated based on Mindlin plate theory to account for the transverse shear deformations *(***cook**, (**1995**)).

Therefore, the shell elements of the three dimensional model were set to take the effects of transverse shear deformations into consideration by modeling them as thick plates.

The Three Dimensional Model preparation started first by judicially meshing the model and carrying out seismic analysis with it. Later, the mesh of the model was refined.
After the final mesh refining, the three dimensional model of the intake tower consists of 1080 shell, 14 beam elements and 76 link elements. The final Three Dimension Model is shown in the **FIGURE 3.15**

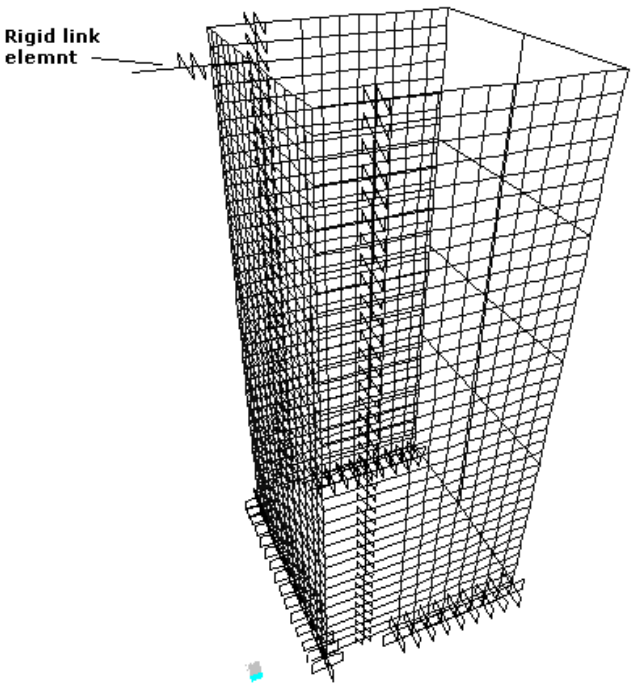

FIGURE 3.15 THREE DIMENSOINAL SHELL MODEL OF THE INTAKE TOWER

The mesh refinement process was conducted for empty reservoir condition. Therefore, there was no need of recalculating of the hydrodynamic load of the reservoir at each round of mesh refining.

However, for seismic analysis of the intake tower with the final meshed model, the hydrodynamic effect were model using Goyal and Chopra's simplified added mass approach. The added masses calculated at a specified level were distributed among the nodes of the Three Dimensional Model.

The other masses lumped at the nodes of the shell element were masses from control room's walls, crane and access foot bridge. The masses from the control room's walls were equally distributed to the top nodes of the upper most shell elements of the three dimensional model. However, the mass from crane was equally divided and lumped on nodes of two shell elements on parallel 1.3m thick walls of the three dimensional model. Moreover, the masses from the access foot bridge were lumped at one end of rigid link whose other end attached to node of shell element closet to the bridge intake tower connections.

The need to introduce the rigid link element arose out of the desire to entertain the effect of distance offset between the connection points and center of the shell element closet to the connection, during seismic analysis of the intake tower.

While modeling the intake tower with shell elements error may creep in (discretizatoin error); mismatch along edge of adjacent shell elements may take place. The software has developed way of preemptively preventing such error by providing meshing parameter like Automatic Edge Constraint. The parameter has been activated, during the seismic analysis using model, in order to cope with the possible mismatch along the edges of the neighboring shell elements

Moreover, the base of the Three Dimensional Model was restrained against translation and rotation in all direction in order to simulate fixed condition at elevation of **913.55m**.This elevation is top of the concrete backfill; in the concrete back fill some part of the intake tower was embedded.

3.8 MODAL ANALYSIS OF THE INTAKE TOWERS' MODELS

The modal analyses of the Beam-Column and the Three Dimensional Models were conducted in order to determine shapes and frequencies of their respective modes of vibrations.

In this study, two modal analysis techniques were considered. Ritz Vector and Eigen Vector are the two possible technique of modal analysis (**CIS**, (**1995**)). **Wilson** (**1995**) demonstrated that dynamic analysis based on the Ritz Vector technique yields more accurate results than results of dynamic analysis obtained using Eigen Vector technique.

Ritz Vector approach yields more accurate results because it generates shapes of modes by taking into account the spatial distribution of the dynamic loading, whereas the Eigen Vectors approach neglects this very important information (**CIS**, **1995**)

Therefore, in this study, Ritz Vector approach has been selected as modal analysis technique during the seismic analysis of the Beam-Column Model as well as the Three Dimensional Model.

3.8.1 MODAL ANALYSIS OF THE BEAM-COLUMN MODEL

The maximum number of the modes of the Beam-Column Model available was equal to its total number of degree of freedoms. The total number of degree of freedom was eighteen. Therefore, the total number of modes of vibrations in the two directions was eighteen. However, not all the eighteen modes contribute considerably to the total seismic response of the Beam-Column Model. So, the number of significant modes must be established from the modal analysis before proceeding to determining the total seismic responses.

		Directions of natural modes' excitations			
		X-Axis		Y-Axis	
Mode NO	Periods (Sec.)	Modal Participating mass ratio of Each mode (%)	Sum of the Ratios	Modal Participating mass ratio of Each mode (%)	Sum of the Ratios
1	0.154	68.1	68.1	0	0
2	0.148	0	68.1	68.1	68.1
3	0.037	22.7	90.8	0	68.1
4	0.036	0	90.8	22.7	90.8

TABLE 3.7 MODAL PARTICIPATING MASS RATIO-(%) FOR THE BEAM-COLUMN MODEL

The number of the significant modes was determined in accordance with the Corps of Engineers guideline which stated that a sufficient mode number should be included such that response quantities calculated during seismic analysis are within 10% of their respective exact values. Alternatively, it may be demonstrated that the participating effective modal masses are at least within 90 percent of the total mass of the structures **(Army of Corps of Engineers, 1999).** For the Beam-Column Model of the intake tower only four out of the eighteen modes, total four mode in both X and Y-axis, were required to satisfy the 90% specification along both X and Y-Axes. The four modes with their periods and participating mass ratios are given in the **TABLE 3.7** while the shapes of the two significant modes, out of four, are portrayed in **FIGURE 3.17** below.

a) 1st MODE along X-Axis **b) 3rd MODE along X-Axis**

FIGURE 3.17 MODE SHAPES OF THE BEAM-COLUMN MODEL

FIGURE 3.17a shows the deflected shape of the first mode in X-direction; the shape of the second is similar to that of first mode but its deflection is in Y-direction. **FIGURE 3.17b** depicts, on its part, the deflected shape of the 3rd mode in X-direction. The deflected shape of the 3nd mode along Y-Axis is also identical to that of along X-Axis.

The determination of the number of significant number of modes was essential for seismic analysis of the intake tower that involves Response Spectrum Method. The determination was not important for seismic analysis of the intake tower that involved Equivalent Lateral Force Method since the method required only a single predominant mode of vibration along X and Y-Axes.

3.8.2 MODAL ANALYSIS OF THE THREE DIMENSOINAL MODEL

As with case of the Beam-Column model, Modal analysis of the Three Dimensional Model was conducted in a bid to obtain the periods and shapes of its mode of vibrations**.**

The Modal analysis was performed utilizing the Ritz vector approach; as result of the analysis, two hundred natural modes were obtained for full reservoir scenario. Their natural periods along with the modal participating ratios are given in **Appendix-C**.

The result, in **Appendix-C**, shows that two hundred modes were required to achieve 100% modal participating mass ratio in X, Y and Z directions. In addition, it depicts that only the

first one hundred fifty three modes are significant to acquire 90% modal participating mass ratio in all of the three directions, as opposed to the significant modes of the Beam-Column Model that are only four in number along two axes. The one hundred fifty three modes were accepted to be the significant modes for seismic analysis of the Three Dimensional Model with **MTHM**.

From the one hundred fifty three significant modes, some were as shown in the **Figure 3.18** below. The first and the second mode, not shown in the figure, involved significant translations in Y and X directions respectively and the twenty fourth significant modes, shown in the figure, contributed primarily to translation along Z-direction.

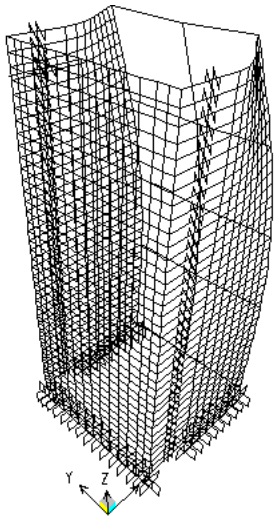

a) THE THIRD MODE

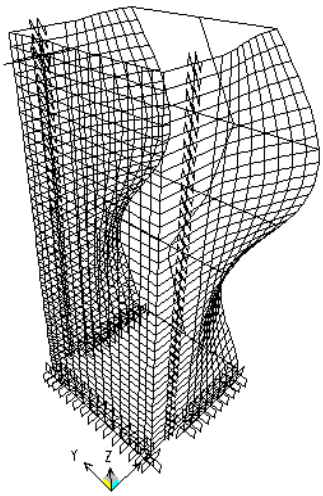

b) THE SIXTH MODE

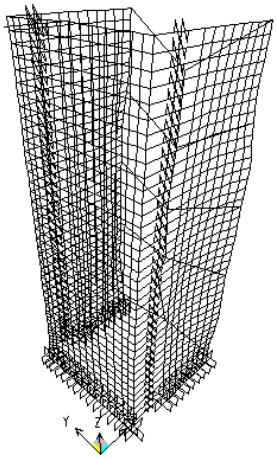

c) THE TENTH MODE

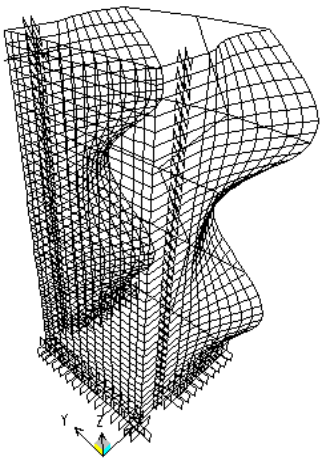

d) THE TWENTY FOURTH MODE

FIGURE 3.18 SOME OF THE SIGNIFICANT MODES' SHAPE OF THE THREE DIMENSOINALMODEL

3.9 Seismic Response Analysis for the Rigid Body Modal Using the Seismic Coefficient Method

The intake tower, modeled as rigid body, was analyzed with the Seismic Coefficient Method (**SCM**) based on theories discussed by **Novak et al**, (**2007**).

As per the theories, the earth quake loads were idealizes as static forces acting on center of gravity of the rigid body model.

The earth quake loads consist of pseudo-static inertia and hydrodynamic loads.

The pseudo-static inertia was determined by multiplying self-weight of the intake tower by the seismic coefficient as stated in Appendix-J.

Moreover, the hydrodynamic load was estimated using a parabolic approximation given by the relation presented in Appendix-J.

As final step, the pseudo-static inertia and hydrodynamic loads were added to obtain the total seismic forces on the intake tower.

This method enjoyed practical application in foreign countries like Japan. In seventies, the Japanese used the method to calculate seismic response of the intake tower, bridges, dams and buildings. However, now days, the method has been categorized as obsolete Novak et al, (2007).

Nevertheless, still, in this country, Seismic Coefficient Method analysis is being used to for detail seismic analysis of intake towers (**WWDSE et al, 2010a**; **WWDSE et al, 2010b** and **WWDSE et al, 2010c**).

Therefore, this study has the intention of comparing the method with more refined method, thereby show their difference quantitatively. From the comparison, the appropriateness or inappropriateness of applicability of the method in our country will be justified.

3.10 SEISMIC ANALYSIS FOR THE BEAM-COLUMN MODEL USING EQUIVELENT LATERAL FORCE METHOD

Equivalent Lateral Force Method (**ELFM**) was employed to conduct seismic analysis of the Beam-Column model based on the frame work indicated by U.S. Army of Corps of Engineers (**U.S Army of Corps of Engineers**, **2007**).

Pursuant to the frame work, the seismic analysis was carried out assuming that the Beam-Column Model deflection was predominantly in its first mode along each X and Y-Axis.

The deflected shapes of the predominant modes, along the two horizontal directions, were determined by extrapolating them from recommended standard deflected shape functions (**U.S Army of Corps of Engineers**, **2007**).

The values of the strandard functoins were produced as function of the ratio of moment of inertias. The ratios are to be obtained by dividing the moment inertia of the top beam element to the moment inertia of bottom elements. The positions of the top and bottom elements are demonstrated in **FIGURE 3.19**.

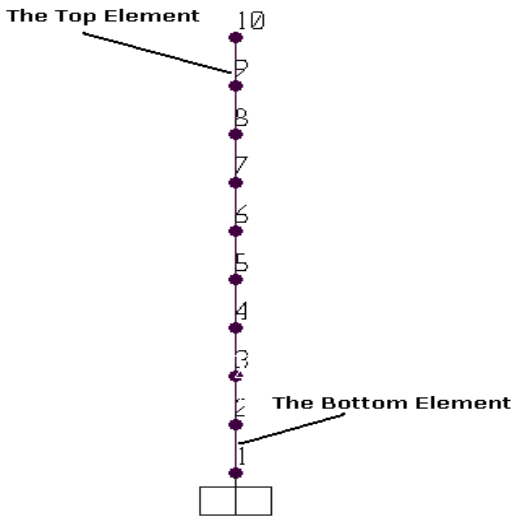

FIGURE 19 TOP AND BOTTOM ELEMNTS OF THE BEAM-COLUMN MODEL

So, the first step in conducting seismic analysis of the Beam-Column Model with Equivalent Lateral Force Method was determination of moment of inertial of the top and the bottom

elements and calculating their ratio. The moment of inertias were calculated about axes through the centroid of the elements and parallel to X-X and Y-Y.

Since the Beam-Column model has uniform cross section throughout its height, all ratios became unity: the Beam-Column model has no tapering.

For lumped mass model with no tapering, the standard deflected shape functions for eleven nodes of a model are given in **TABLE-D**, **APPENDIX-D**. From the table, identical standard deflected shape function was selected for both deflections in X and Y-Axes because of the moment of inertia ratio in both directions were unity.

The number of nodes of the Beam-Column Model differed from that of that of the standard deflected shape function. Therefore, the deflected shapes function of the Beam-Column Model were extrapolated from the Standard deflected Shape functions whose values were given at eleven nodal points and at equal intervals. The extrapolated deflected shapes functions of the Beam-Column Model are listed in the **TABLE 3.8** below.

Location of the nodes as Fraction of L	**Shape Functions (Φ_{r-1})**	
1.0L	Φ_{10-1}	**1.00**
0.89L	Φ_{9-1}	**0.847**
0.78L	Φ_{8-1}	**0.695**
0.67L	Φ_{7-1}	**0.548**
0.56L	Φ_{6-1}	**0.407**
0.44L	Φ_{5-1}	**0.279**
0.33L	Φ_{4-1}	**0.167**
0.22L	Φ_{3-1}	**0.080**
0.11L	Φ_{2-1}	**0.022**
0.0L	Φ_{1-1}	**0.000**

TABLE 3.8 THE DEFLECTED SHAPE FUNCTOINS FOR THE BEAM-COLUMN MODEL

The extrapolations of the deflected shape functions of the Beam-column Model, were followed by determination of the stiffness constants in the directions of X and Y-Axes. To do so, the following relationships were employed:

$$\mathbf{K_X} = \mathbf{Coef_X}\,\frac{\mathbf{EI_{topX}}}{\mathbf{L^3}}$$

$$\mathbf{K_Y} = \mathbf{Coef_y}\,\frac{\mathbf{EI_{topY}}}{\mathbf{L^3}}$$, where $\mathbf{L}$ = total height of intake tower

$\mathbf{K_X}$ =stiffness constant in the direction of X-Axis,

$\mathbf{K_Y}$ = stiffness constant in the direction of Y-Axis,

$\mathbf{Coef_X}$ =coefficient of stiffness constant in the direction of X-axis,

$\mathbf{Coef_y}$ =coefficient of stiffness constant in the direction of Y-axis,

$\mathbf{I_{topX}}$=moment inertia of the top element about X-Axis,

$\mathbf{I_{topY}}$ =moment inertia of the top element about Y-Axis, and

$\mathbf{E}$ =Modulus of Elasticity of concrete.

The coefficient of stiffness constants, along with the standard deflected functions, are also given as function of the moment inertia ratios in **TABLE-D**, **APPENDIX-D**. So they were directly taken from the table in the Appendix. In the table, for the moment inertia ratio of unit, the coefficient of stiffness for both axes is given as **3.09**.

Similarly, the stiffness constants were selected from the table for moment inertia ratio of unity. The selected stiffness constants and other parameters are short listed in **TABLE 3.9** below.

	unit	Values
E	GPa	36.8
L	m	27.45
$Coef_x$	-	3.901
I_{topx}	m^4	1576.52
K_x	KN/m	10,941,987.32
$Coef_y$	-	3.901
I_{topy}	m^4	1735.03
K_y	KN/m	12,042,141.09

TABLE 3.9 STIFNESS CONSTANTS ALONG BOTH X AND Y AXES

Selection of the stiffness constants from the **TABLE B-1**, in the **APPENDIX**-**B**, may be regarded as being analogous to determination of modal stiffness of the fundamental mode of The Beam-Column. In the same manner, as per the framework, **ELFM** requires determination of single lumped masses which are analogous to modal mass calculation in Modal Analysis method.

Therefore, the single lumped masses along both X and Y Axes, analogous to the generalized modal masses, were calculated using the relationships written below:

$$\mathbf{m_x} = \sum_{r=1}^{10} \mathbf{m_{xr}}\, \mathbf{\Phi^2_{r-1}}\text{, and}$$

$$\mathbf{m_y} = \sum_{r=1}^{10} \mathbf{m_{yr}}\, \mathbf{\Phi^2_{r-1}}\text{, Where}$$

$\mathbf{m_x}$ = the single mass along X-axis,

$\mathbf{m_y}$ =the single mass along Y-axis,

$\mathbf{m_{xr}}$ =total mass lumped at $\mathbf{r^{th}}$ node and along X-Axis,

$\mathbf{m_{yr}}$ =total mass lumped at $\mathbf{r^{th}}$ node and along X-Axis, and

$\mathbf{\Phi_{r-1}}$ = is the deflected shape function of $\mathbf{r^{th}}$ node.

Below here, **TABLES 3.10** and **3.11** summarize steps of calculation of the single lumped masses.

m_{xr}(KN-s^2/m)		Φ_{r-1}		$(\Phi_{r-1})^2$	$(m_{xr})\ ((\Phi_{r-1}))^2$
m_{x1}	799.69	Φ_{10-1}	1	1	799.69
m_{x2}	1588.61	Φ_{9-1}	0.847	0.717	1139.683
m_{x3}	1572.49	Φ_{8-1}	0.695	0.483	759.551
m_{x4}	1569.8	Φ_{7-1}	0.548	0.300	471.417
m_{x5}	1553.68	Φ_{6-1}	0.407	0.165	257.365
m_{x6}	1524.12	Φ_{5-1}	0.279	0.078	118.639
m_{x7}	1475.74	Φ_{4-1}	0.167	0.023	41.157
m_{x8}	1389.75	Φ_{3-1}	0.08	0.006	8.894
m_{x9}	1255.38	Φ_{2-1}	0.022	0.000484	0.607
m_{x10}	1637.93	Φ_{1-1}	0	0	0
				$m_x = \Sigma(m_{xr})((\Phi_{r-1}))^2 =$	**3597.00**

TABLE 3.10 SINGLE LUMED MASS ALONG X-AXIS

m_{yr}(KN-s^2/m)		Φ_{r-1}		$(\Phi_{r-1})^2$	$(m_{xr})*(\Phi_{r-1})^2$
m_{Y1}	805.06	Φ_{10-1}	1.00	1.00	805.06
m_{Y2}	1608.5	Φ_{9-1}	0.847	0.717	1153.952
m_{Y3}	1597.75	Φ_{8-1}	0.695	0.483	771.753
m_{Y4}	1583.24	Φ_{7-1}	0.548	0.300	475.4533
m_{Y5}	1561.74	Φ_{6-1}	0.407	0.165	258.700
m_{Y6}	1540.24	Φ_{5-1}	0.279	0.078	119.894
m_{Y7}	1486.49	Φ_{4-1}	0.167	0.023	41.457
m_{Y8}	1400.5	Φ_{3-1}	0.08	0.006	8.963
m_{Y9}	1271.5	Φ_{2-1}	0.022	0.000484	0.615
m_{Y10}	1643.3	Φ_{1-1}	0	0	0
$m_y^* = \Sigma(m_{yr})((\Phi_{r-1}))^2 =$					**3635.849**

TABLE 3.11 SINGLE LUMPED MASS ALONG Y-AXIS

Next, the single masses along with the stiffness constants and coefficient of stiffnesses, in both directions, were employed to calculate natural periods of The Beam-Column Model. As

result of the calculations, the natural period for excitation in X and Y Axes were found to be **0.114s** and **0.109s** respectively.

The natural periods, in turn, were used to read their corresponding spectral accelerations from elastic response spectrum which was displayed in **FIGURE 3.4**.The numerical value of spectral ordinate corresponding to **0.114s** was read to be **7.51m/s²**(S_{xA}) while that corresponding to **0.109s** was **7.36m/s²**(S_{yA}).

After determination of the spectral ordinates, the following step was the calculation of the modal mass participation factors (PF_{x1} and PF_{y1}): PF_{x1} was modal participation factor along X-Axis and PF_{y1} was along Y-Axis **.**The formula here below was provided by U.S Army of Corps of Engineers to be employed for the calculation of the factors.

$$PF_{x1} = \frac{L_{x1}}{m_x} \text{ and } PF_{y1} = \frac{L_{y1}}{m_y},$$

$$\text{Where } L_{x1} = \sum_{0}^{L} m_{xr}\,\Phi_{r-1} \text{ and } L_{y1} = \sum_{0}^{L} m_{yr}\,\Phi_{r-1}.$$

Accordingly, the modal participation factors for excitation along Y-Axis and X-Axis were calculated but they were found to be almost identical; the numerical value of the identical factor was **1.54**.

The details of the participation factor calculations, based on the relationships, are given in **APPENDIX-E**.

The intension of determination of deflected shapes, natural periods, modal participation factors and spectral ordinate so far was, to prepare inputs for estimations of seismic response quantities such as, bending moment, shear forces, and lateral forces at the nodes of the Beam-Column Model. So, in the coming paragraphs the procedures of estimations of the seismic response would be discussed in a detail.
To begin with, the lateral forces at the nodes of the Beam-Column Model were calculated making use of the following relations:

$$F_{xr} = PF_{x1}\,m_{xr}\,S_{xA}\,\Phi_{r-1}, \text{ and}$$

$$F_{yr} = PF_{y1}\,m_{yr}\,S_{yA}\,\Phi_{r-1}$$

Where,

$\mathbf{F_{xr}}$ is lateral force at $\mathbf{r^{th}}$ node in the X-direction and $\mathbf{F_{yr}}$ is lateral force at the same node level but in the Y-direction.

The results of the calculations are placed in the **TABLE 3.12** constructed below.

r	Φ_{r-1}	m_{xr} (KN-s^2/m)	m_{yr} (KN-s^2/m)	F_{xr} (KN)	F_{yr} (KN)
10	1	799.69	805.06	9248.735	9124.872
9	0.847	1588.61	1608.5	15561.855	15441.981
8	0.695	1572.49	1597.75	12639.601	12586.129
7	0.548	1569.8	1583.24	9949.140	9833.901
6	0.407	1553.68	1561.74	7313.355	7204.464
5	0.279	1524.12	1540.24	4917.949	4870.697
4	0.167	1475.74	1486.49	2850.276	2813.695
3	0.08	1389.75	1400.5	1285.841	1269.906
2	0.022	1255.38	1271.5	319.417	317.057
1	0	1637.93	1643.3	0	0

TABLE 3.12 THE LATERAL FORCES AT r^{th} NODE OF THE BEAM-COLUMN MODEL

Examination of **TABLE 3.12** reveals that at a node the lateral forces or the inertia forces in X-Axis and Y-Axis are almost identical.

These lateral forces, in their part, were used to calculate the shear forces at their respective nodes. At the node, in each direction, the shear force was calculated by summing all of the lateral forces above the node. The following equations assisted the process of summing up the later forces:

$$\mathbf{V_{xr}} = \sum_{\mathbf{n=r+1}}^{\mathbf{10}} \mathbf{F_{x\,n}} \;, \mathbf{V_{yr}} = \sum_{\mathbf{n=r+1}}^{\mathbf{10}} \mathbf{F_{y\,n}} \text{ , where}$$

$\mathbf{V_{xr}}$ = the summed up shear force in X-direction at $\mathbf{r^{th}}$ node,

$\mathbf{V_{yr}}$ =is the summed up shear force in X-direction at $\mathbf{r^{th}}$ node,

$\mathbf{F_{x\,n}}$ =is lateral force above $\mathbf{r^{th}}$ node in X-direction, and

$\mathbf{F_{y\,n}}$ =is lateral force above $\mathbf{r^{th}}$ node in Y-direction.

Displayed in **FIGURE 3.20** is the envelop vales of the shear forces along X and Y-Axis obtained based on the above equations.

The shear forces value along X-axis and Y-axis are almost equal. The equality is attributed to the fact that the design ground motions of both directions are identical; moreover, the moments inertias about the respective axes are also similar and masses lumped in both direction are almost identical too.

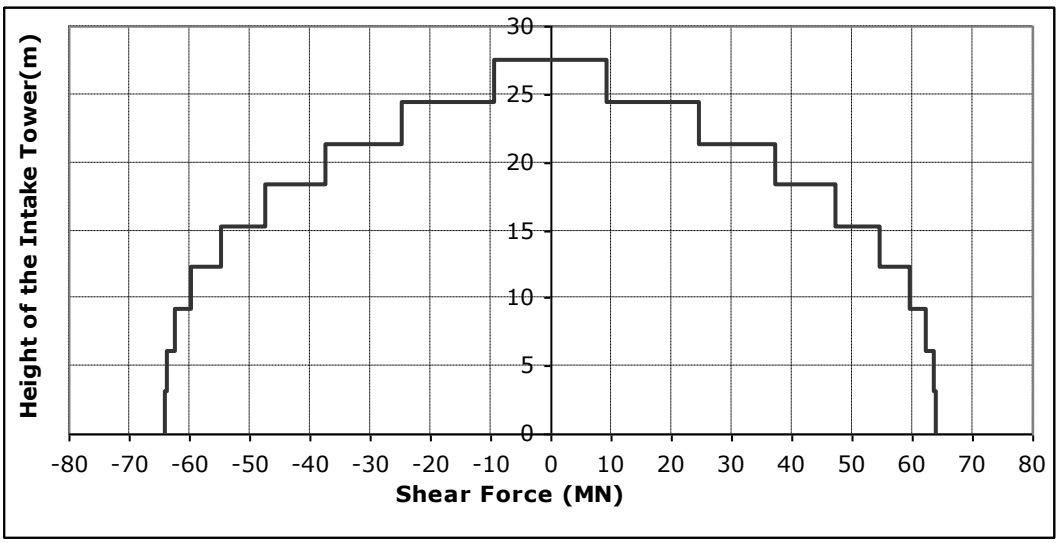

FIGURE 3.20 ENVELOPS OF SHEAR FORCES ALONG X and Y-AXIS FOR ELF

Next to shear forces, at each node of the Beam-Column Model, the response quantities estimated were the bending moments.

The estimation of the bending moments was conducted using the relationship stated below:

$$\mathbf{M_{xr} = M_{x(r+1)} + V_{x(r+1)} \times \Delta h}\ ,\ \mathbf{M_{yr} = M_{y(r+1)} + V_{y(r+1)} \times \Delta h}$$ where

$\mathbf{M_{xr}}$ **=**is the bending moment about X-X and at $\mathbf{r^{th}}$ node level,

$\mathbf{M_{yr}}$ = is the bending moment about Y-Y and at r^{th} node level, and

$$\mathbf{\Delta h} = (\text{height of } \mathbf{(r+1)^{th}} \text{ node}) - (\text{height of } \mathbf{r^{th}} \text{ node}).$$

Diagrammatically in the form of envelops, the estimated bending moments are indicated on the **FIGURE 3.21** below,

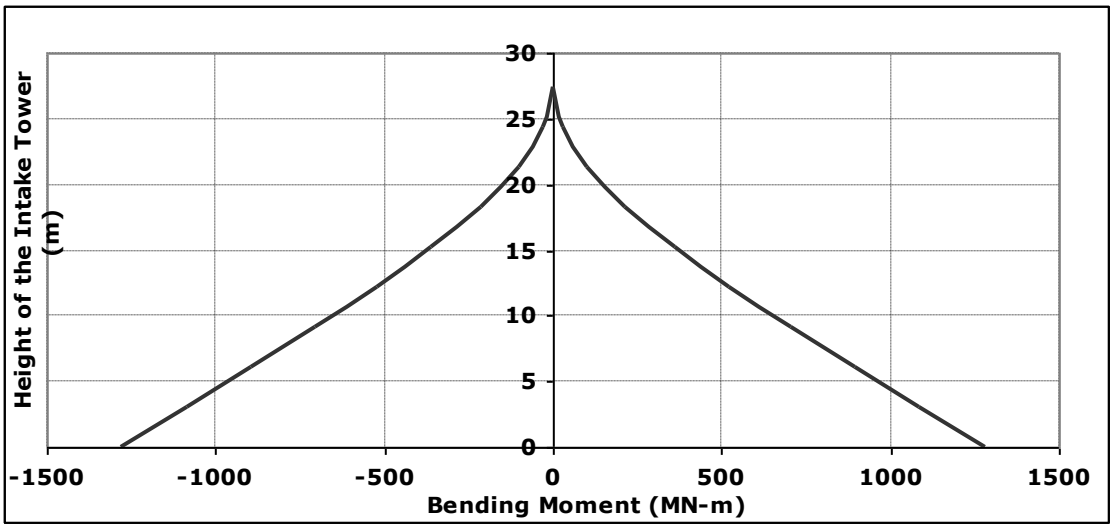

FIGURE 3.21 ENVELOPS OF BENDING MOMENT ABOUT X-X AND Y-Y FOR ELF

Due to the same argument produced for the equality of the shear forces acting along X and Y Axes, the value of bending moment about X-X and Y-Y are found to be practically equal.

Torsional moments at the nodes of the Beam-Column Model were computed as final step of using **ELFM** to analyze seismic response of intake tower.

The torsional moments at the nodes were computed as sum of the incremental moments above the node. The torsional moments were obtained by multiplying the lateral forces above the node with its eccentricity from the center of rigidity (**U.S Army Corps of Engineers, 2003b**).

Since the eccentricity of the simplified cross-section of the intake tower existed only in Y-direction, the lateral forces in X-direction alone, therefore, believed to gave rise to torsional moments.

As result, the lateral forces in X-direction were used to compute the torsional moments at the nodes of the Beam-Column Model.

The results of the computation of the torsional moments at the nodes of the Beam-Column are shown in the **TABLE 3.13** here below.

Node number (**r**)	Eccentricity (m)	$\mathbf{F_{xr}}$ (KN)	Torsional Moment at $\mathbf{r^{th}}$ Node (KN-m)	Sum of Torsional Moments at $\mathbf{r^{th}}$ Node (KN-m)
10	7.12	9248.735	65850.991	65850.991
9	6.45	15561.855	100373.964	166224.955
8	6.45	12639.601	81525.425	247750.380
7	6.45	9949.140	64171.953	311922.332
6	6.45	7313.355	47171.138	359093.471
5	6.45	4917.949	31720.771	390814.242
4	6.45	2850.276	18384.283	409198.525
3	6.45	1285.841	8293.676	417492.200
2	6.45	319.417	2060.242	419552.443
1	6.45	0.000	0.000	419552.443

TABLE 3.13 TORSONAL MOMENT OF BEAM-COLUMN AS COMPUTED WITH ELFM

Observation of the seismic response quantities revealed that they, except the torsional moments, posses one common resemblance. The common resemblance was that at each node the X and Y components of each response quantity have almost equal numerical values.

3.11 SEISMIC RESPONSE ANALYSIS FOR THE BEAM-COLUMN MODEL USING RESPONSE SPECTRUM METHOD

The other method applied to analyze the seismic response of the intake tower was Response-Spectrum Method (**RSM**). The analysis was accomplished using the Beam-Column Model which was used to idealize the intake tower.

Unlike **ELFM**, the seismic analysis was conducted with aid of the software package, SAP2000.

The software was provided with inputs that were estimated or determined in the previous sections. The inputs are:

- Concrete properties.
- Two orthogonal horizontal design ground motions.
- Number of Significant Modes.
- Hydrodynamic added masses.

In addition to above mentioned items, other parameters were also predefined to the software as preprocessing activity.

For instance, the modal combination rule was selected for the analysis based on the disparity or closeness of the natural periods.
For modal excitations along X-Axis, the spacing between the natural periods **0.154s** and **0.035s** found to be wide. Similarly, for modal excitation along Y-Axis, the spacing between **0.148s** and **0.036s** also found to be wide too. Consequently, the rule Square Root of Sum of Squares (**SRSS**) was selected for modal combination, since the natural periods were widely spaced. Moreover, the same rule was chosen for the directional combination of the response quantities computed with **RSM**.

After the predefinition, the software was activated to run the analysis. The results of the analysis, shear forces and bending moments are reported as envelop values in **FIGURE 3.22** up to **3.24**.
FIGURE 3.22 shows envelop of nodal bending moments about X-X and Y-Y.

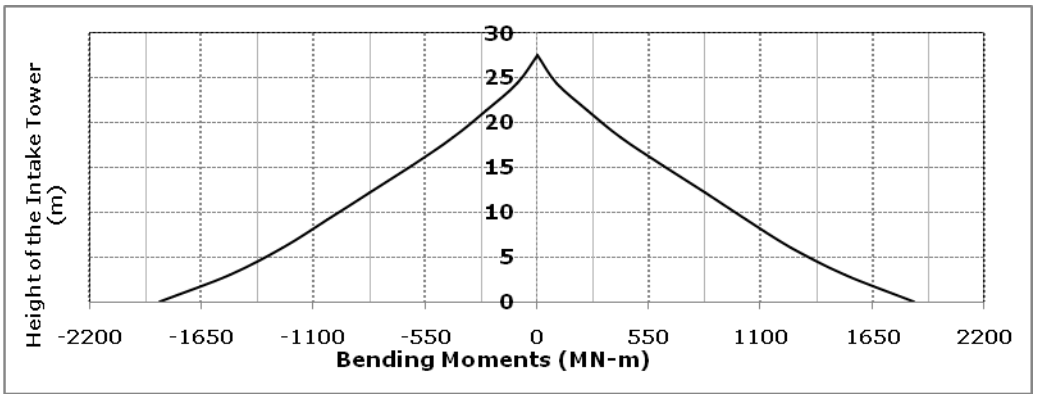

FIGURE 3.22 ENVELOP OF BENDING MOMENTS ABOUT X-X AND Y-Y FOR RSM

Figure 3.23 shows envelop of nodal shear along X and Y-Axes.

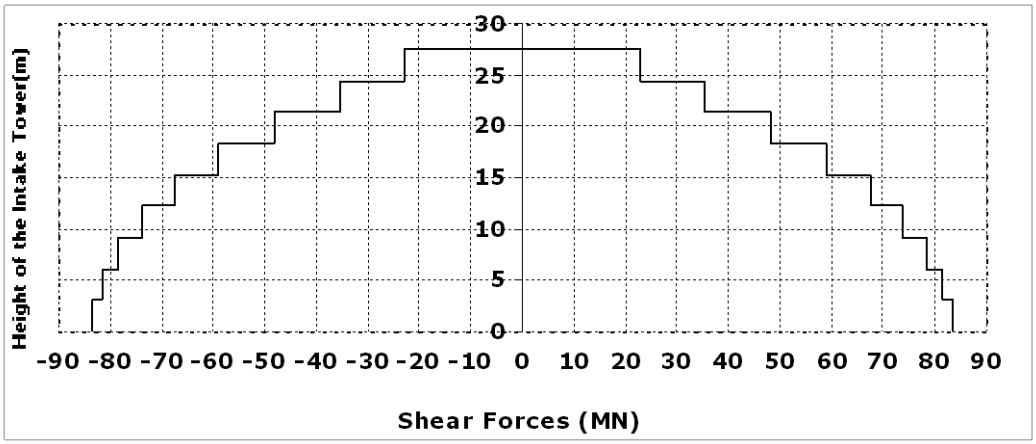

FIGURE 3.23 ENVELOP OF NODAL SHEARFORCES ALONG X AND Y-AXES FOR RSM

Torsional moments were determined at the along the height of the Beam-Column Model following series of steps.

As first step, modal response quantities along X-Axis, such as natural periods, spectral accelerations, and deflected shape were obtained from The Modal Analysis. The quantities would be used in a view to know the inertia forces of each made at all nodes. Modal responses quantities along Y-axis were not considered for determination of the torsional moment, because the geometry of the simplified model was symmetrical about this axis.

The natural periods from the Modal Analysis were used to read the spectral accelerations from elastic specific response spectrum established in previous section.

In second step, participation factor of transitional modes in the X-direction were calculated. The details of the calculations are explained in **TABLE E-1**, and **TABLE E-2**, **APPENDIX-E**.

In the third steps, the Lateral forces at the nodes of the Beam-Column Model were calculated separately for each of the transitional modes.

The lateral forces were calculated bearing in mind the directions of the nodal displacements. The direction of the nodal displacements indicated the directions of the nodal inertial forces i.e. the direction of the lateral forces.

Finally, the lateral forces would be used to calculate the torsional moments. For one of the modes, at a node, the torsional moments were calculated by multiplying the lateral force with its eccentricity from shear center. The torsional moments calculated in the same manner for other nodes at higher elevations would be added to the torsional moment to give the total torsional moment at the node under the consideration.

so, the torsional moment of each modes were modal combined to give the total torsional moment of the Beam-Column as analyzed with **RSM** .Because of wide spacing between the natural periods ,**SRSS** had been selected for the modal combination.

The combined torsional moments of the Beam–Column Model analyzed with **RSM** are put in **TABLE 3.14** and are also shown diagrammatically in **FIGURE 3.24**

Node No	Torsional Moments of First mode (KN-m)	Torsional Moments of Third mode (KN-m)	Combined Torsional Moments (KN-m)
10	75033.821	-21235.279	77980.84
9	191970.380	-39769.535	196046.531
8	288874.225	-38634.722	291446.323
7	367732.434	-19187.049	368232.652
6	427160.174	14487.549	427405.782
5	468874.975	56247.404	472236.712
4	494965.831	97711.171	504518.232
3	508432.393	130139.494	524823.575
2	512700.648	147171.680	533405.528
1	512700.648	147171.680	533405.528

TABLE 3.14 MODALLY COMBINED TORSOINAL MOMENTS FOR RSM

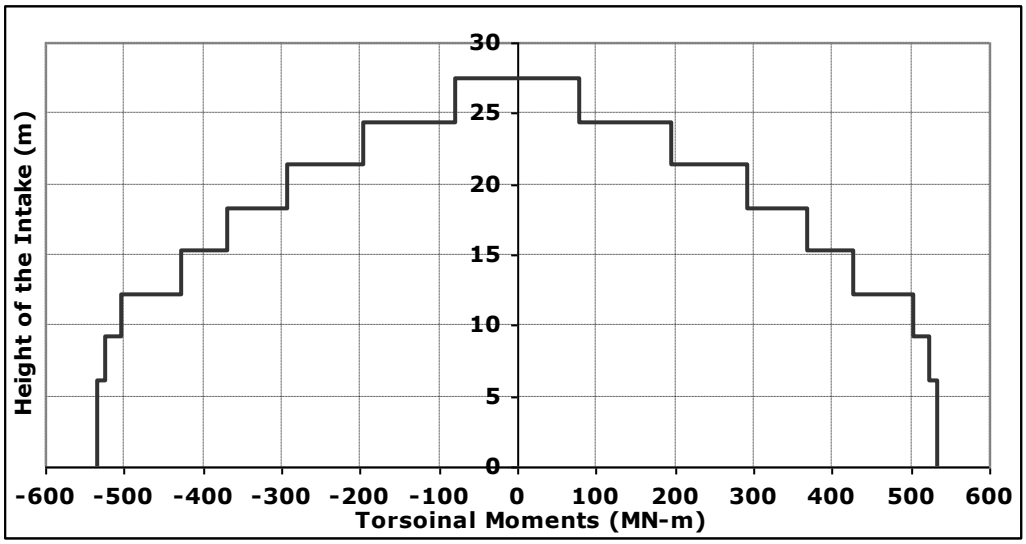

FIGURE 3.24 ENVELOP OF MODALLY COMBINED TORSOINAL MOMENTS FOR RSM

In addition to the Beam-Column model, the three dimension modeled was analyzed with **RSM** in order to learn about the impact of type of the model on the out put of the seismic analysis of the intake tower with the method under consideration. The result pointed out that the impact could be considered negligible since the magnitude difference between response quantities found to be **7.6**% at maximum. The result of the seismic analysis, shear forces, of both **3D** and Beam-Column models estimated with **RSM** is demonstrated in **APPENDIX-H**, in **FIGURE-H-1** and **FIGURE-H-2**; and in **Table-H**.

3.12 SEISMIC RESPONES ANALYSIS FOR THE SHELL ELEMENT MODEL USING MODAL-TIME HISTORY METHOD

The third method, with which the seismic analysis of intake tower was evaluated, in this study, was the Modal-Time History Method (**MTHM**).

The Modal-Time History of analysis of the intake tower was too conducted with help of Computer program, SAP2000.

To this software, parameters and the model determine in previous sections were defined as an act in prepossessing stage. The parameters and the model are: concrete dynamic properties, Three Dimension Model, design ground motions, number of significant modes and hydrodynamic added mass.

Concrete dynamic properties, discussed in **section 3.7.1** and listed in **TABLE 3.4**, were defined for shell and beam elements that constitute the Three Dimensional Model.

In order to represent the reservoir water inertia force on the model during the analysis, the equivalent hydrodynamic added mass estimated in **section 3.7.2** were lumped to the nodes of the model.

In addition, the sets of suite of ground accelerations developed in **section 3.6** were encoded to the computer program as input to idealize earthquake loads' envelops.

Under the time history analysis, the Ritz vector approach was again selected to run the modal analysis of the Three Dimensional Models. Moreover, the numbers of significant modes decided previously in **section 3.8.2** was endorsed and given to the program.

The decision regarding the number of significant modes was made with aim of capturing the predominant modal response for the Modal-Time History analysis of the intake tower, thereby obtaining sufficient seismic responses magnitude from time history analysis of the intake tower (**U.S. Army Corps of Engineers, 2003a**).

The other parameter predefine to the software was time-step which was used for discretizing the generated suite ground acceleration time-histories. Concerning the time-step, the software documentation stated that the Modal-Time History incorporated in it is secure from numerical instability that results from improper selection of time-step. However, it recommended that time-steps as small as or smaller than one tenth of the period of the fundamental mode can be selected to obtain reliable seismic analysis out put.

In case of this study, the one tenth of the period of the fundamental mode is equal to **0.022s**, but the time step **0.01s** smaller than recommended by the software has been selected as time-step for the Modal-Time History Analysis. In fact, **0.01s** is a time step at which the artificial ground accelerations are recorded.

After defining the inputs mentioned here above, the software was activated to run seismic analysis of the intake tower with the Modal-Time History method so as to compute envelops of maximum and minimum section forces.

The maximum and minimum section forces along the intake tower height were computed from stresses at bottom joints of the shell elements; the bottom of the shell elements made up the section. To do so, especial capability of Sap2000 to compute group joint forces has been invoked.

As the result, section forces or shear forces along X and Y directions, and bending moments about X-X, Y-Y directions and torsional moment about Z-Axis were obtained.

Diagrams for the shear forces in X and Y directions due to sets of the artificial ground acceleration time histories **ACC-1**, **ACC-2**, and **ACC-3** are displayed in **FIGURES 3.25** and **3.26.** Similarly, diagrams for the bending moments about X-X, Y-Y directions, and

torsional moment about Z-Axis due to the same artificial ground acceleration time-histories are shown too in **FIGURES 3.27**, **3.28** and **3.29** respectively.

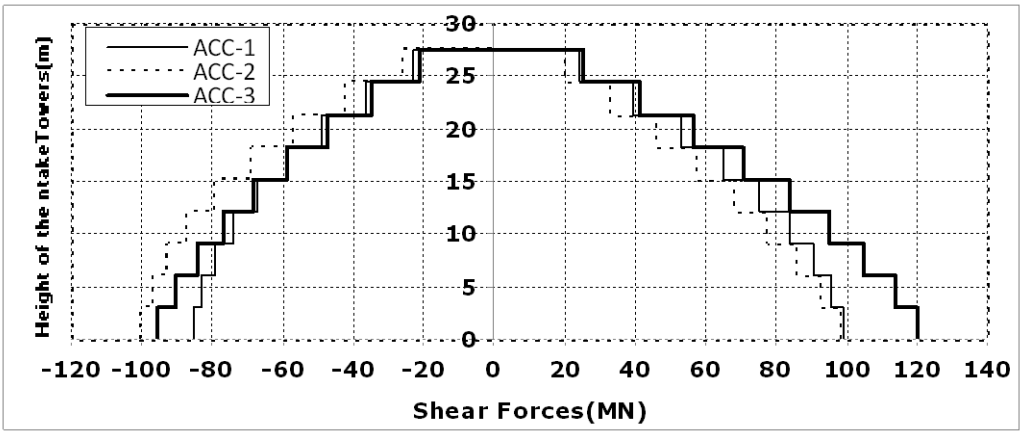

FIGURE 3.25 DIAGRAMS OF ENVELOPS OF SHEARFORCES IN X-AXIS FOR MTHM

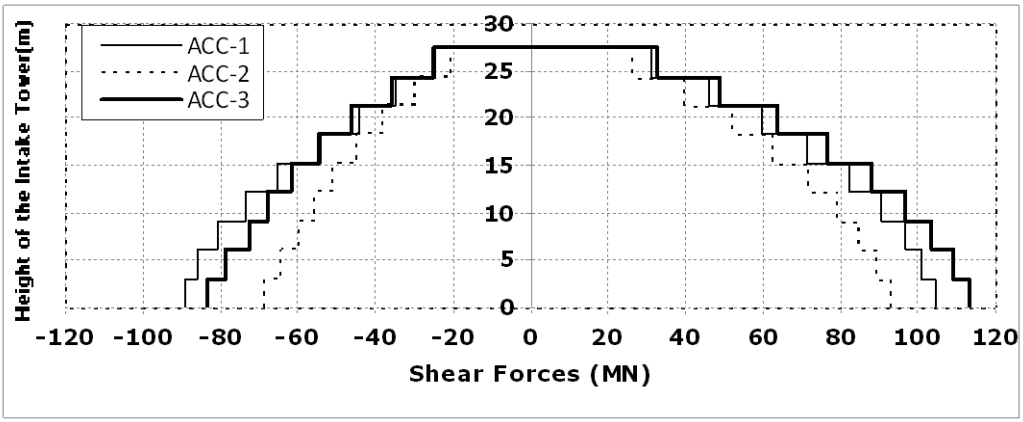

FIGURE 3.26 DIAGRAMS FOR ENVELOPS OF SHEARFORCES IN Y-AXIS FOR MTHM

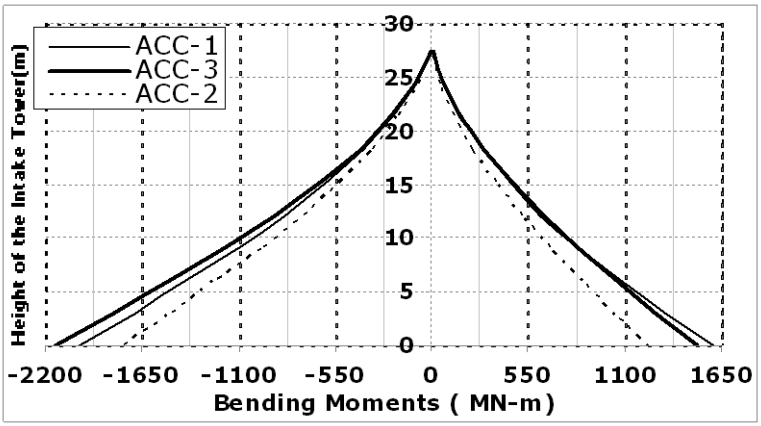

FIGURE 3.27 DIAGRAMS OF ENVELOPS OF MOMENTS ABOUT X-X FOR MTHM

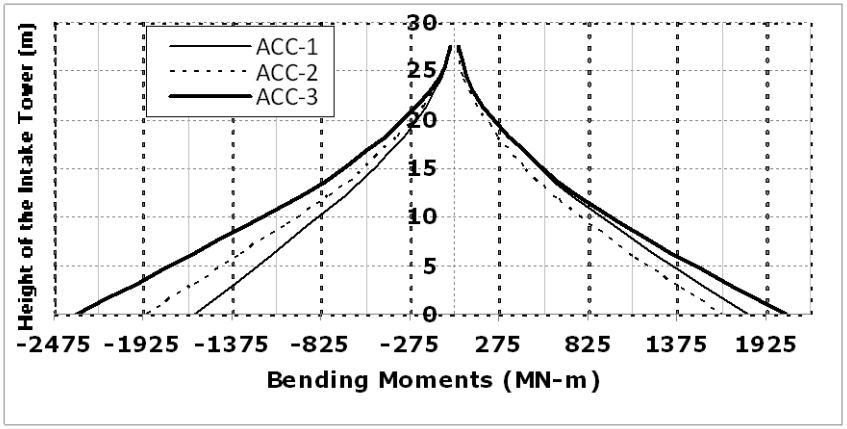

FIGURE 3.28 DIAGRAMS OF ENVELOPS OF MOMENTS ABOUT Y-Y FOR MTHM

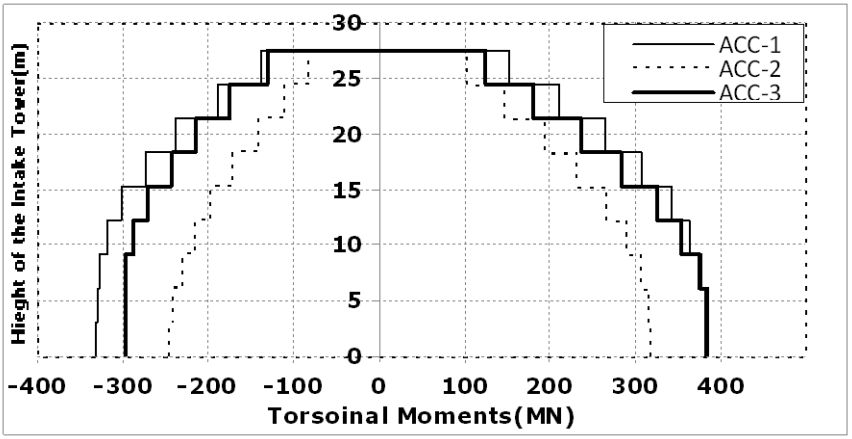

FIGURE 3.29 DIAGRAMS OF ENVELOPS OF MOMENTS ABOUT Z-AXIS FOR MTHM

3.12.1 DETERMINATOIN OF ENVELOP VALUES

In each of the **FIGURES 3.25** up to **3.29**, the shear forces and bending moments due to artificial earthquake loads (**ACC-1**, **ACC-2** and **ACC-3**) have been presented by a set of three shear force and a set of three bending moment diagrams along and about each global direction.

The outer boundaries of these diagrams were taken as envelop values of the response quantities along or about the global direction.

For instance, The envelop values of the shear force in Y-direction consists of the shear force diagram due to **ACC-1** ,on the left in **FIGURE 3.26**; and the shear force diagram

due to **ACC-3**,on the right in **FIGURE 3.26**.The resulting envelop values of the shear force along Y-axis is shown in **FIGURE 3.31.**

In similar fashions, envelop values of the other response quantities along or about each global direction were decided and put in **FIGURE 3.30** up to **FIGURE 3.34.**

The envelop value were used to represent the response quantities computed with **MTHM** and to compared them with their respective response quantities estimated with the other two methods. The details of the comparisons will be discussed in the coming sections.

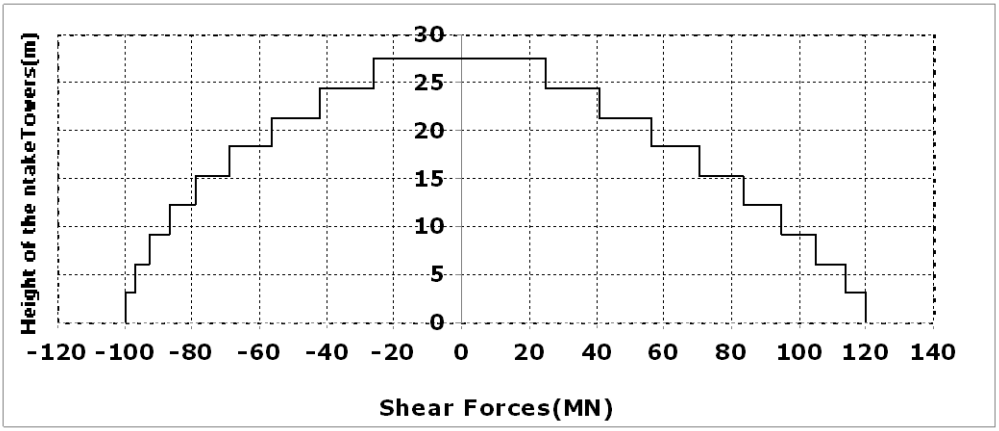

FIGURE 3.30 RPERSENTATIVE SHEARFORCE ENVELOP (IN X-DIRECTOIN)

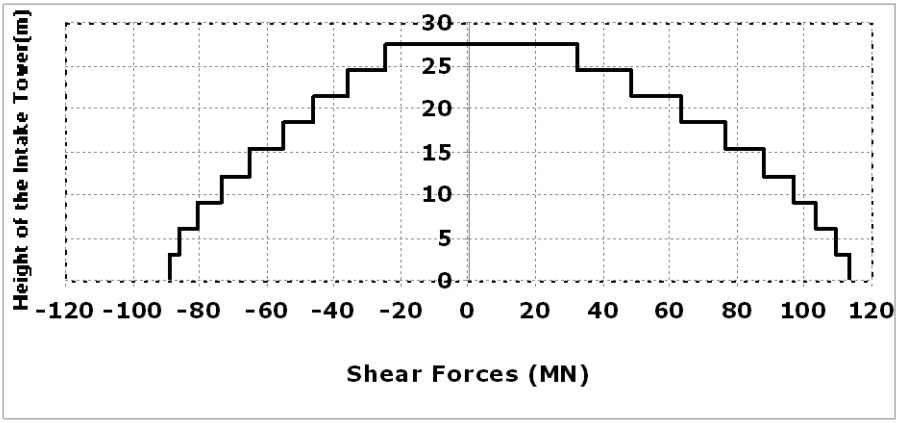

FIGURE 3.31 REPERSENTATIVE SHEARFORCE ENVELOP (IN Y-DIRECTOIN)

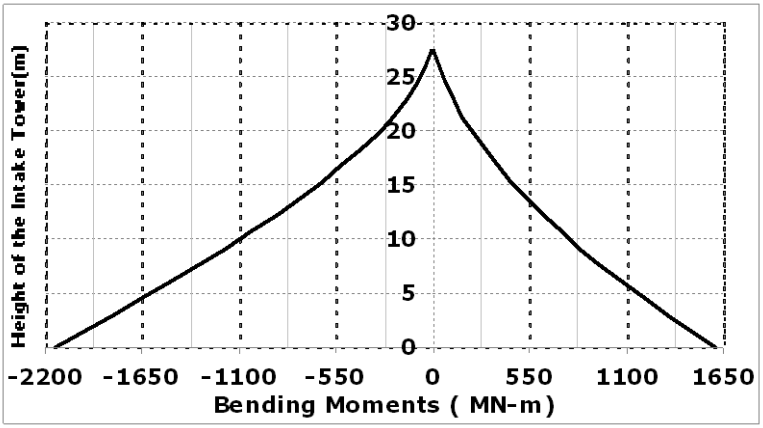

FIGURE 3.32 REPERSENTATIVE BENDING MOMENT ENVELOP (ABOUT X-X)

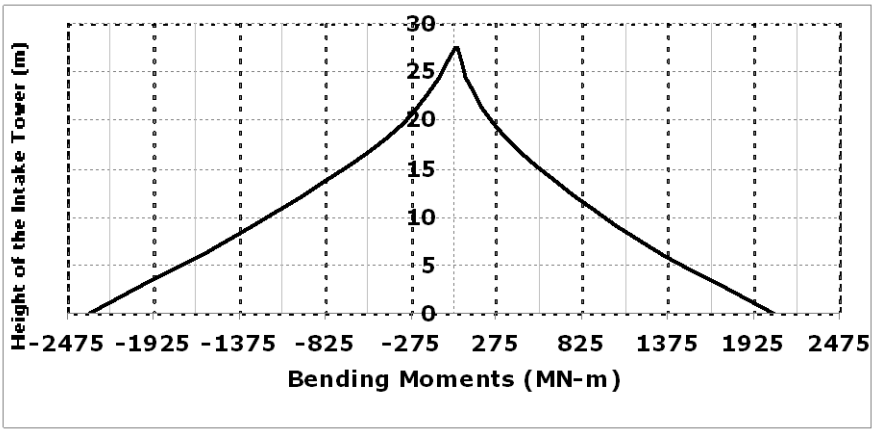

FIGURE 3.33 REPERSENTATIVE BENDING MOMENT ENVELOP (ABOUT Y-Y)

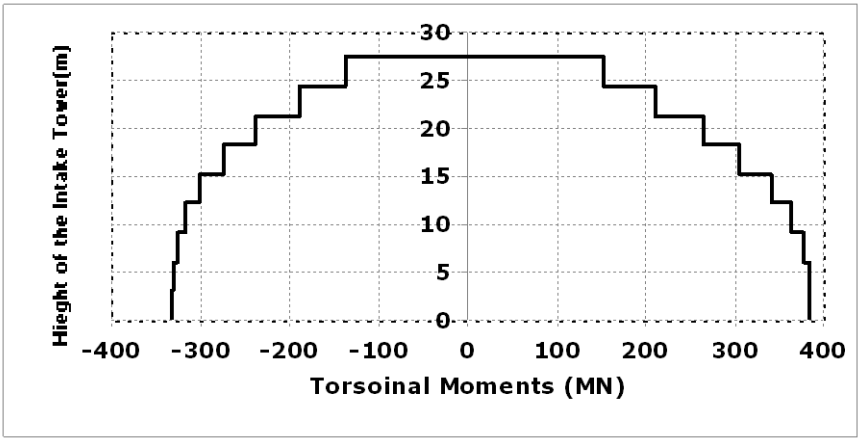

FIGURE 3.34 REPERSENTATIVE TORSOINAL BENDING MOMENT ENVELOP (ABOUT Z-AXIS)

The analysis result of seismic analysis of the 3D presented so far has been estimated using only **MTHM**. So, now, it seems important to check whether the analysis results remain the same for **RSM**.

Therefore, the **3D** model has been analyzed with **RSM** and one of the results has been compared with corresponding result of **MTHM**. The comparison demonstrated that the difference of the seismic analysis result was negligible. The comparison was made diagrammatically using shear forces computed along the height of the intake. The diagrammatical comparison is shown in **APPENDIX-I**, in **FIGURE-I**.

4.0 COMPARATIVE STUDIES AMONG RESPONSE QUANTYITIES COMPUTED WITH THE THREE METHODS

The four Methods of seismic analysis were evaluated based on the comparison made among their respective response quantities coupled with engineering judgments. The comparison was made qualitatively using graphical presentations of complete response quantities along the height of the intake tower. In addition, the shears and moments at base of the intake tower were also compared quantitatively to look closely at the difference in magnitudes of response quantities computed with the methods.

Taking one of the categories of response quantity at a time, the response quantities were compared in order to evaluate the methods in detail and categorically. The response quantity categories included shear forces, moments about X-X and Y-Y, and torsional moments.

4.1 COMPARATIVE STUDY BASED ON SHEARFORCES

The first type of response quantity considered as base for evaluating the four methods analysis was, the complete shear forces, in X-Axis and Y-Axis, along the height of the intake tower ;and base shears at the bottom of the intake tower.

The comparison using the complete shear force along the height of the intake tower is demonstrated graphically in **FIGURE 4.1** and **FIGURE 4.2**

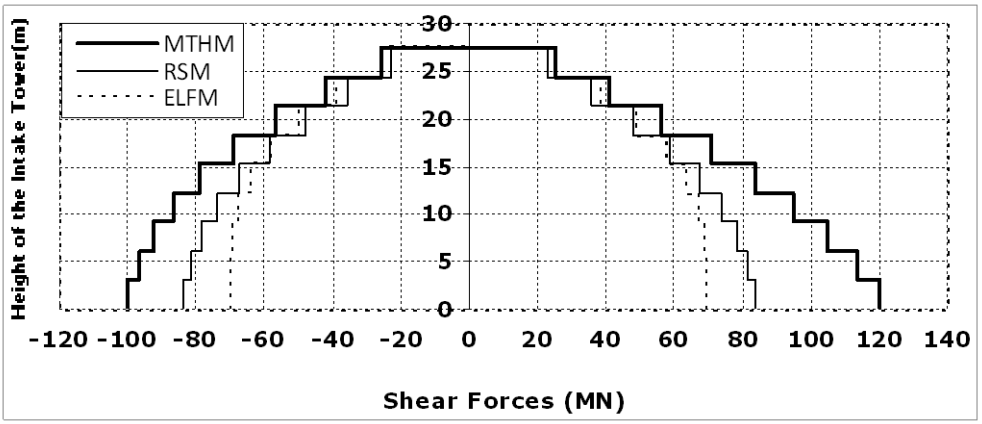

FIGURE 4.1 SHEAR FORCES IN X-AXIS FOR ELFM, RSM AND MTHM

FIGURE 4.1 demonstrates that the biggest shear force values along the height of the intake are the ones computed with **MTHM** and followed by **RSM** and **ELF** in decreasing orders.

At base of the intake tower in the X-direction, the shear force value for **MTHM** is at maximum **1.7** times the shear force value for **ELF** and **1.4** times the shear force value for **RSM**; moreover, Shear force value for **RSM** is larger than the shear force value for **ELF** by factor of **1.2.**

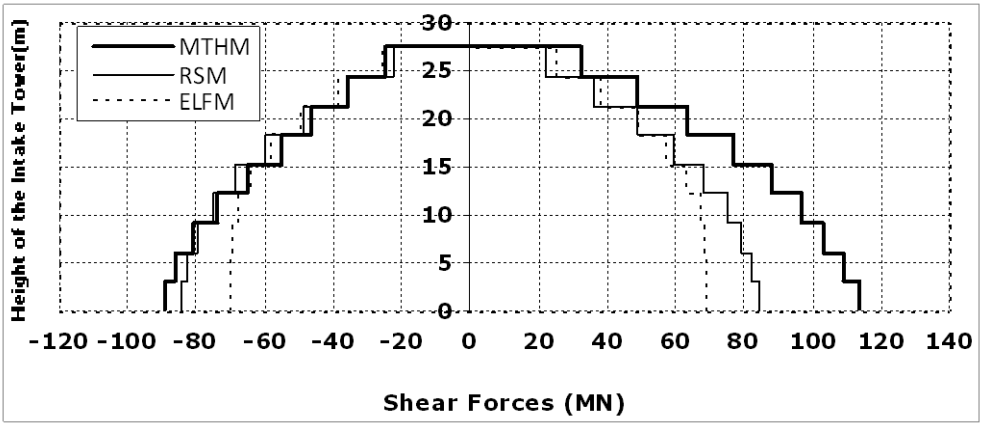

FIGURE 4.2 SHEAR FORCES IN Y-AXIS FOR ELFM, RSM AND MTHM

In the same way, in Y-direction along the height of the intake tower **FIGURE 4.2** portrays that **MTHM** yields shear force value that almost envelops the shear force values for **ELF** and **RSM**.

FIGURE 4.2 depicts that, at base of intake tower, the shear force value for **MTHM** in negative y-direction is about **1.3** times the value of **RSM** and is about **1.6** times the shear force value of **ELF**; nevertheless, the shear force value for **MTHM** in positive y-direction is equal to that of **RSM** and is as big as **1.2** times the value of **ELF**.

Therefore, from shear force perspective, **MTHM** produced shear force values that appreciably exceed the shear force values computed with **ELF** or **RSM** for the case of intake tower consider in this study.

4.2 COMPARATIVE STUDY BASED ON MOMENTS ABOUT X-X AND Y-Y

The third seismic response quantity essential to evaluate the Equivalent lateral Force, Response Spectrum, and Modal Time History methods was bending moments about X-X, Y-Y and Z-Z directions.

For the purpose of the evaluations, the conventions for the senses of the bending moments were determined with right hand rule. The direction to which the thumb indicates is taken to be positive in sense but the reverse direction is considered as negative sense.

FIGURE 4.3 used to illustrate, diagrammatically, the comparison made among the bending moment values for the three methods along the height of the intake tower.

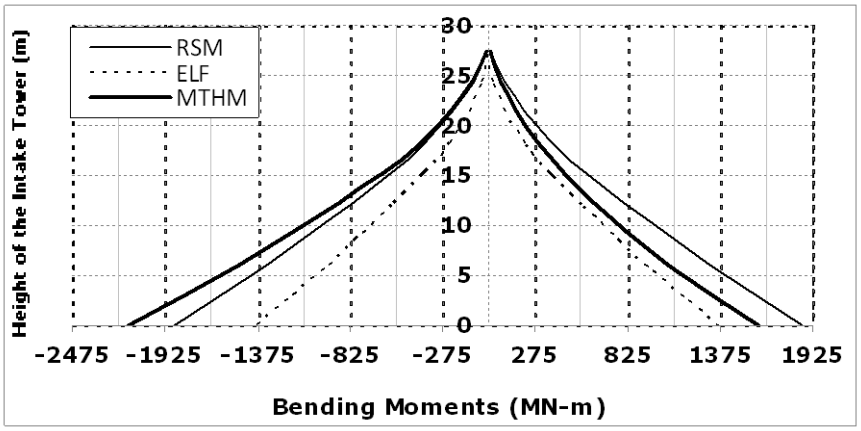

FIGURE 4.3 BENDING MOMENTS ABOUT X-X FOR ELFM, RSM AND MTHM

As per **FIGURE 4.3**, for the bending moment about X-X and with positive sense, along the full height of the intake tower, **MTHM** gives values less than that of **RSM**; however, the negative bending moment diagram for **MTHM** lies above the negative bending diagram for **RSM.** For **ELFM**, the magnitude of negative and positive bending moments about X-X is the smallest of all along the height of intake tower.

At base of the intake tower, the magnitude of the negative bending moment about X-X from **MTHM** is bigger than that from **RSM** by factor of **1.1**, and is also larger than that from **ELFM** by factor of **1.6**.

Furthermore, at base of the intake tower, the value of bending moment with positive sense and about Y-Axis for **MTHM** was found out to be approximately equal to the bending moment value for **RSM** in the same sense and direction. At same location, in the same

axis and direction, the bending moment magnitude calculated with the former method topped the magnitude of bending moment for **ELFM** in order of **1.5**.

FIGURE 4.4 compares the bending moment value along the height of the intake tower and about Y-Axis for the three methods of Seismic analysis. For both negative and positive senses, the figure shows that the diagrams drawn for bending moment value computed with **ELFM** and **RSM** are almost enveloped in by the diagram sketched for bending moment value computed with **MTHM**.

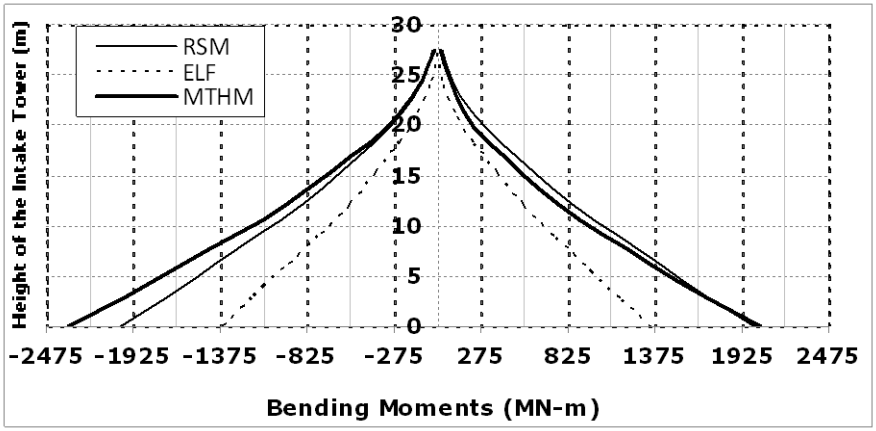

FIGURE 4.4 BENDING MOMENTS ABOUT Y-Y FOR ELFM, RSM AND MTHM

Generally speaking, in the negative sense and in both directions, the bending moment values for seismic load on the intake tower estimated with **MTHM** were the largest in magnitude as compared to bending moment value due to the other two methods.

In the positive sense in both directions, the bending moment values computed with **RSM** are greater than that of **MTHM**. However, for the same sense and direction, the bending moment values for **RSM** exceeded the bending moment value of **ELFM**.

4.3 COMPARATIVE STUDY BASED ON THE TORSOINAL MOMENTS

The last response quantity considered in evaluating the method of seismic analysis of intake was torsional moment. Along the height of the intake tower, **FIGURE 4.5** portrays that the **RSM** yields almost the biggest torsional moment magnitude followed by that of **ELFM**, and the smallest magnitude of torsional moment calculated was with **MTHM**.

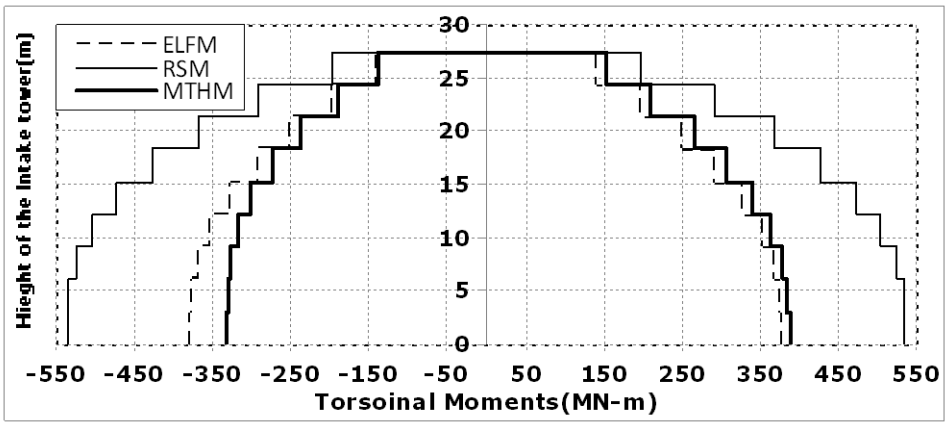

FIGURE 4.5 TORSOINAL MOMENT ABOUT Z-AXIS FOR ELFM, RSM AND MTHM

The Torsional moment magnitude computed with **MTHM** was the lowest; however, the same method had been used to calculate the biggest magnitude of shear forces. When **MTHM** yielded the biggest shear force magnitude, it was anticipated that the method would result in the biggest magnitudes of torsional moments too. On the contrary to what was expected, **MTHM** produced torsional moment with the smallest magnitude.

The assumptions made during the computation of the torsional moments with **ELFM** and **RSM** was responsible for what happened in contradiction to the anticipation.

The assumption was that the shear flow in the simplified section of intake tower was similar to the shear flow of thin walled sections.

Based on the assumption, the eccentricity of the intake tower section was conservatively estimated for computation of the torsional moment with **ELFM** and **RSM**.
However, For **MTHM** there was no need of assuming the shear flow pattern in the section and calculating the corresponding shear center, since the three dimensional finite element model for **MTHM** automatically and more accurately accounts for the eccentricity (**CIS**, **1995**).To put things in a nut shell, the reasons why torsional moments for **RSM** and **ELFM** were bigger than the torsional moments due **MTHM**, were due to the assumption of shear flow pattern similar to that of the thin wall section and the associated conservative eccentricity estimations.

4.4 SUMMARY OF THE COMPARATIVE STUDIES

The **TABLE 4.1** below is used to demonstrate, in summary, the comparison made between the response quantities computed with **MTHM** and with the other three methods (**ELFM, SCM** and **RSM**). The table shows the shear forces and bending moments' ratios of **ELFM, SCM** and **RSM** at the base of the intake tower to those of **MTHM** at the same location.

Response Quantities	Directions	Methods of Analysis	Factor by which **MTHM** exceeded the Method of Analysis	
			minimum	maximum
Shear forces	Along X-Axis	**ELFM**	1.4	1.7
		RSM	1.1	1.4
		SCM	2.7	3.3
	Along Y-Axis	**ELFM**	1.2	1.6
		RSM	1	1.3
		SCM	2.5	3.4
Bending Moments	About X-Axis	**ELFM**	1.2	1.6
		RSM	0.9	1.1
		SCM	3.8	4.8
	About Y-Axis	**ELFM**	1.5	1.7
		RSM	1.0	1.2
		SCM	5.4	4.7

TABLE 4.1 SUMMARIES OF THE FACTORS BY WHICH RESPONSE QUANTITIES COMPUTED WITH MTHM EXCEEDED THE RESPOSE QUANTY DETERMINED WITH RSM AND ELFM

The magnitude of the ratios varied from method to method, from response quantities to response quantities. Even, for the same method and response quantity the ratios varied form direction to direction. For instance, the bending moment ratio for **RSM** about Y-axis was **1.2**; the ratio about X-axis for the same response quantity was **1.1**.However, generally speaking, **MTHM** produced response quantities with the the biggest magnitudes when compared with the other four methods.

The table shows that the magnitudes of shear forces and bending moments computed with **MTHM** at the base of the intake tower, at maximum, differed significantly from the magnitudes of shear forces and bending moments estimated with **ELFM** and **SCM**.

Similarly, the shear force magnitude of **MTHM** deviated from those of **RSM** but not as significant as it was for those of **ELFM** and **SCM**. However, regarding the bending moments magnitudes, the difference between **MTHM** and **RSM** is balanced one.

The response quantity not entered in the table is torsion; however, the following statement can be written to summarize the comparison made among the method of analysis based on the response quantity: the magnitude of torsion computed with **MTHM** is lowest of the magnitude of torsion estimated with the other two methods.

5.0 CONCLUSOIN AND RECOMMENDATOINS

This study was conducted with the aim of evaluating four seismic analysis methods of intake towers, **Equivalent Lateral Force** (**ELFM**), **Response Spectrum** (**RSM**), **Seismic Coefficient** (**SCM**) and **Modal Time-History** (**MTHM)** methods .The evaluation included examination of extent with which the magnitudes of response quantities computed with the **ELFM**, **SCM** or **RSM** differed from the magnitudes of the response quantities calculated with the more refined method (**MTHM**).

Moreover, the study was carried out with special interest of comparing magnitudes of seismic response quantities computed with **SCM** to magnitudes of response quantities estimated with **MTHM**. The interest arose because **SCM** was being used for detail seismic analysis of intake tower in this country, Ethiopia. So, this study has aim of commenting on the acceptability of using **SCM** for practical application.

5.1 CONCLUSOINS.

In this study, generally, after the evaluation of the seismic analysis methods of the intake tower, it was concluded that the extent of the magnitude differences between the seismic response quantities computed with the refined methods (**MTHM)** and the other three methods were appreciable. In other words, **SCM**, **ELFM** and **RSM** underestimated magnitudes of seismic response quantities of squat free-standing intake towers. Especially, **SCM** underestimated the magnitudes adversely than **ELFM** and **RSM** did, but; the underestimation of **RSM** was not as intense as it was for **ELFM** or **SCM**.

Therefore, detail seismic analysis of free-standing squat intake tower shall preferably and satisfactorily be carried out with the refined method (**MTHM)**. The Usage of the method is emphasized for final seismic analysis and subsequent detail design of the intake tower.

Nevertheless, using **SCM**, **ELFM** or/and **RSM** for detail seismic analysis of the structure is not acceptable, so design offices shall refrain from using them for practical applications. Particularly, the design offices, in Ethiopia, should abandon their current practice of applying **SCM** for detail seismic analysis of squat free-standing intake towers. However, the three methods (**SCM**, **ELFM** and **RSM**) are recommendable for seismic analysis of intake tower in preliminary study stages. Even, during the detail seismic analysis stage, **SCM** can still be used for stability analysis of the intake tower.

Alternatively, the approach towards seismic analysis of the intake tower may be performed progressively. The progressive analysis starts from **SCM** or **EFLM**, proceeds to **RSM**, and finalizes with **MTHM**. The progressive analysis will be observed at least for detail and final seismic analysis of the intake tower.

Moreover, the study found out that the magnitudes of response quantities computed using **SCM**, **ELFM**, **RSM** and **MTHM** do not depend on the type of models used to idealize the squat free-standing intake tower. Rather, the magnitudes rely on the type of method used to perform the seismic analysis.

5.2 RECOMMENDATOINS.

This study is limited to evaluation of elastic analysis methods of squat free-standing intake towers. As result, the conclusions of this study hold true only for elastic seismic analysis methods and for squat free-standing intake towers.

Therefore, similar investigations are required in order to extend the conclusions of this study to slender free-standing as well as inclined intake towers, and to inelastic seismic analysis methods of the intake towers.

REFERENCES

1. **Chopra A. K., 1995:**
   Dynamics of Structures. Renticel Hall, New Jersey, USA.
2. **CIS, 1995:**
   SAP2000 Analysis Reference and User Guide (1995). Computers and Structures, Inc., Berkeley, California, USA.
3. **Cook R.D., 1995:**
   Finite Element Modeling for Stress Analysis. John Wiley & Sons, Inc., New York, USA.
4. **Dowrick D.J.,1978:**
   Earthquake Resistant Design. A Wiley-Interscience publication, New York, USA.
5. **EBCS-1,1995:**
   Basis of design and actions on structures, Ministry of Works and Urban Development, Adiss Ababa, Ethiopia.
6. **EBCS-2,1995:**
   Structural use of Concrete, Ethiopian Building Code Standard. Ministry of Works and Urban Development, Adiss Ababa, Ethiopia.
7. **EBCS-8,1995:**
   Design of Structures for Earthquake Resistance, Ethiopian Building Code Standard. Ministry of Works and Urban Development, Adiss Ababa, Ethiopia.
8. **Eurocode-8 part-1, 2003:**
   Design of Structures for Earthquake Resistance. Europeans Code for seismic actions and rules for buildings and other structures.
9. **Farrar C.R. and Duffey T.A. ,1995:**
   Evaluation of an existing bridge's modal properties using simplified finite element analysis. Internet:
   <http: // www.osti.gov/bridge/product.biblio.jsp?osti_id=188885>.
10. **FEMA 451, 2006:**
    2003 NEHRP Recommended Provision for Seismic Regulations for New Building and other Structures and Accompanying Commentary. Internet:
    <http: // www.wbdg.org/ccb/DHS/fema451.pdf>.
11. **Geophysical Observatory, 2005:**
    Seismic Hazard Analysis at Kesem Dam Site. Science Faculty, Adiss Ababa University, Ethiopia

12. Johnson W. G., Chiarito V.P. and Holmes R. L., 1993:

Seismic Analysis of Arkabuta Intake-out let structures. Internet:
< http://oai.dtic.mil/oai/oai?verb=getRecord&metadataPrefix=html&identifier=ADA259276>.

13. Mid-South Design and Research Institute, 2008:

Main Dam Design Optimization Report. Water Works Design and Supervision Enterprise, Adiss Ababa, Ethiopia.

14. Mosley B., Bungey J. and Hulse R.,2007:

Reinforced concrete design to Eurocode-2.Palgrave Macmillan, New York, U.S.A.

15.Novak P., Moffat A., Nalluri C. and Nurayanan R., 2007:

Hydraulic Structutrs .Taylor and Francis, London and Newyork.

16. Spyrakos C.C. and Chaojin Xu, 1997:

Soil-Structure-Water Interactions of Intake-Outlet Towers Allowed to Uplift. Internet: **<**http: // linkinghub.elsevier.com/retrieve/pii/S0267726196000346**>**.

17. Vidot A.L, Suarez L. E., Mathew E. E., and Sharp M.K.,2004a:

Seismic Analysis of Intake towers Considering Multiple-Support Excitations and Soil-structure Interactions Effects. Internet:
<http: // handle.dtic.mil/100.2/ADA427787>.

18. Vidot A.L, Suarez L. E., Mathew E. E., and Sharp M.K.,2004b:

Seismic Analysis of Intake towers Considering Multiple-Support Excitations and Soil-structure Interactions Effects. Internet:
<http: // handle.dtic.mil/100.2/ADA427787>.

Citing, Daniell W.E. and Taylor C.A. (1994): Full Scale Dynamic Testing and Analysis of a Reservoir of Intake tower. Earthquake Engineering and Structural Dynamics 23, 1219-37.

19. Vidot A.L, Suarez L. E., Mathew E. E., and Sharp M.K.,2004C:

Seismic Analysis of Intake towers Considering Multiple-Support Excitations and Soil-structure Interactions Effects. Internet:
<http: // handle.dtic.mil/100.2/ADA427787>.

Citing, Goyal A. and Chopra A., 1989b: Hydrodynamic and Foundation Interaction Effects in dynamics of Intake towers. Journal of Structural Engineering Mechanics 115(7), 1393-1435.

20. U.S Army of Corps of Engineers, 1995:

Earthquake Design and Evaluation for Civil Works, Engineering Manual 1110-2-1806. Internet:

<http:// 140.194.76.129/publications/eng-regs/er1110-2-1806/entire.pdf>.

21. U.S Army of Corps of Engineers, 1999:

Response Spectra and Seismic Analysis for Concrete Hydraulic Structures, EngineeringManual1110-2-6051.Internet:

<http://40.194.76.129/publications/eng-manuals/em1110-2-1110-2-6051/entire.pdf>.

20. U.S. Army Corps of Engineers, 2003a:

Time-History Dynamic Analysis of Concrete Hydraulic Structures, Engineering Manual 1110-2-6051.Internet:

< http://140.194.76.129/publications/eng-manuals/em1110-2-6051/entire.pdf>.

21. U.S Army Corps of Engineers, 2003b:

Structural Design and Evaluation of outlet Works. Engineering Manual 1110-2-2400. Internet:

<http://140.194.76.129/publications/eng-manuals/em1110-2-2400/entire.pdf >.

22. U.S. Army of Corps of Engineers, 2007a:

Earthquake Design and Evaluation of Concrete Hydraulic Structures, Engineering Manual 1110-2-6053.Internet:

< http://140.194.76.129/publications/eng-manuals/em1110-2-6053/entire.pdf>

23. U.S. Army of Corps of Engineers, 2007b:

Earth Quake Design and Evaluation of Hydraulic Structures, Engineering Manual 1110-2-6053. Internet:

<http://140.194.76.129/publications/eng-manuals/em1110-2-6053/entire.pdf>.

Citing, Wilson, E.L. and Button M., 1982:Earthquake Engineering and Structural Dynamics; Smedy, W. and Der Kiureghian A., 1985: Earthquake Engineering and Structural Dynamics.

24.U.S. Army of Corps of Engineers, 2007c:

Earthquake Design and Evaluation of Concrete Hydraulic Structures, Engineering Manual 1110-2-6053.Internet:
< http://140.194.76.129/publications/eng- manuals/em1110-2-6053/entire.pdf>.
Citing, Bruhwieler, 1990: Dam Engineering.

25.Wilson E.L., 1995:

Three-Dimensional Static and Dynamic Analysis of structures**.** Internet:

< http://ww.csi.berkeley.com>.

26. WWDSE and TAHAL Group, 2010a:

Gilgel Abbay Dam Project: Final Detail Design Report. Water Workers Super Vision Enterprise, Adiss Abab, Ethiopia.

27. WWDSE and TAHAL Group, 2010b:

Megech Dam Project: Final Detail Design Report. Water Workers Super Vision Enterprise, Adiss Abab, Ethiopia.

28. WWDSE and TAHAL Group, 2010c:

Rib Dam Project: Final Detail Design Report. Water Workers Super Vision Enterprise, Adiss Abab, Ethiopia.

APPENDIX-A

DETREMINATOIN OF EQUIVELENT HYDRODYNAMIC ADDED MASSES ON THE BEAM-COLUMN MODEL

Table-A HYDRODYNAMIC ADDED MASSES LUMPED AT THE NODES OF BEAM-COLUMN MODEL

				Directions of earthquake excitations	
				Along X-axis	Along Y-axis
Trial No	Number of nodes	Node №	Node elevation(m)	Added mass (KN-s^2/m)	Added mass (KN-s^2/m)
1	3	1	0	1354.43	1370.55
		2	9.15	2676.61	2708.85
		3	18.3	2450.87	2499.24
		4	27.45	1128.69	1160.94
2	5	1	0	1354.43	822.33
		2	5.49	1615.64	1634.99
		3	10.98	1567.27	1586.61
		4	16.47	1489.87	1499.54
3	7	5	21.96	1189.96	1257.68
		6	27.45	464.37	532.10
		1	0	580.26	587.17
		2	3.92	1153.61	1170.88
		3	7.84	1139.79	1157.06
		4	11.76	1105.25	1125.98
		5	15.68	1036.17	1081.07
		6	19.6	946.37	991.27
		7	23.52	773.68	794.40
		8	27.45	324.67	331.58
4	9	1	0	451.48	456.85
		2	3.05	892.20	912.09
		3	6.1	876.08	901.34
		4	9.15	873.39	886.83
		5	12.2	857.27	865.33
		6	15.25	827.71	843.83
		7	18.3	779.33	790.08
		8	21.35	693.34	704.09
		9	24.4	558.97	575.09
		10	27.45	236.49	241.86

APPENDIX-B

CALCULATOIN OF THE LUMPED MASS DUE TO INTAKE TOWER, CONTROL-ROOM, CRANE LOAD AND BRIDGE

TABLE-B TOTAL LUMPED MASS FROM INTAKE TOWER, CONTROL-ROOM, CRANE AND BRIDGE

Trial No	Number of elements	Node №	Node elevation(m)	Intake Tower's Lumped Masses (KN-s^2/m)	Control Room's, Bridge's, and Crane's lumped Masses (KN-s^2/m)
1	3	1	0	1019.24	-
		2	9.15	2038.49	-
		3	18.3	2038.49	-
		4	27.45	1019.24	1053.23
2	5	1	0	626.77	-
		2	5.49	1253.54	-
		3	10.98	1253.54	-
		4	16.47	1253.54	-
		5	21.96	1253.54	-
		6	27.45	626.77	1053.23
3	7	1	0	447.53	-
		2	3.92	895.06	-
		3	7.84	895.06	-
		4	11.76	895.06	-
		5	15.68	895.06	-
		6	19.6	895.06	-
		7	23.52	895.06	-
		8	27.45	447.53	1053.23
4	9	1	0	348.21	-
		2	3.05	696.41	-
		3	6.1	696.41	-
		4	9.15	696.41	-
		5	12.2	696.41	-
		6	15.25	696.41	-
		7	18.3	696.41	-
		8	21.35	696.41	-
		9	24.4	696.41	-
		10	27.45	348.21	1053.23

APPENDIX-C

DETERMINATOIN OF SIGNIFICANT MODES OF THE THREE

DIMENSOINAL MODEL

TABLE-C THE TWO HUNDREND SIGNIFICANT MODES OF THREE DIMENSOINAL MODEL

		Directions of Natural Mode Excitations					
		X-Axis		Y-Axis		Z-Axis	
Mode NO	Periods (Sec.)	Participating mass ratio (%)	Sum of the ratios	Participating mass ratio (%)	Sum of the ratios	Participating mass ratio (%)	Sum of the ratios
1	0.223694	0.000	0.000	41.015	41.015	0.000	0.000
2	0.182517	65.277	65.277	0.000	41.015	0.002	0.002
3	0.122831	0.000	65.277	12.055	53.071	0.000	0.002
4	0.115734	0.000	65.277	0.213	53.284	0.001	0.003
5	0.110871	0.242	65.519	0.004	53.288	0.912	0.914
6	0.07691	0.000	65.519	1.589	54.876	0.000	0.914
7	0.065624	0.000	65.519	2.631	57.507	0.000	0.914
8	0.05886	0.023	65.541	0.000	57.507	0.001	0.915
9	0.055401	0.022	65.563	0.000	57.507	0.004	0.919
10	0.050806	0.001	65.564	0.566	58.073	0.000	0.919
11	0.05054	0.079	65.643	0.001	58.074	0.000	0.919
12	0.048932	0.893	66.536	0.001	58.075	0.000	0.919
13	0.046272	4.813	71.349	0.023	58.098	0.016	0.935
14	0.044569	4.715	76.064	0.100	58.198	0.009	0.945
15	0.044449	0.034	76.098	9.562	67.760	0.000	0.945
16	0.04423	4.496	80.594	0.034	67.794	0.006	0.951
17	0.043487	6.854	87.448	0.036	67.830	0.003	0.954
18	0.040501	0.042	87.490	0.001	67.831	0.000	0.954
19	0.038946	0.094	87.585	0.000	67.831	0.000	0.954
20	0.0368	0.014	87.598	0.000	67.832	0.023	0.977
21	0.035423	0.000	87.598	1.254	69.086	0.000	0.977
22	0.033846	0.000	87.599	0.013	69.098	0.000	0.978
23	0.033568	0.011	87.609	0.002	69.101	0.000	0.978
24	0.032794	0.014	87.624	0.000	69.101	75.051	76.028
25	0.030806	0.000	87.624	0.003	69.103	0.000	76.028
26	0.030248	0.001	87.625	0.000	69.103	0.239	76.268
27	0.027593	0.004	87.628	0.020	69.123	0.449	76.717
28	0.027472	0.000	87.628	4.561	73.684	0.000	76.718
29	0.026916	0.003	87.631	0.004	73.688	0.599	77.317

30	0.025589	0.000	87.631	0.538	74.226	0.000	77.317
31	0.025057	0.000	87.631	0.058	74.284	0.000	77.317
32	0.024822	0.312	87.944	0.000	74.284	0.034	77.351
33	0.023728	0.000	87.944	0.198	74.482	0.000	77.351
34	0.023512	0.369	88.313	0.001	74.483	0.000	77.351
35	0.022531	0.100	88.412	0.000	74.483	0.003	77.355
36	0.021336	2.054	90.466	0.000	74.483	0.015	77.370
37	0.02127	0.008	90.474	0.000	74.483	0.000	77.370
38	0.02093	0.000	90.475	0.164	74.648	0.000	77.370
39	0.020448	0.017	90.491	0.003	74.651	0.000	77.371
40	0.020218	0.867	91.358	0.000	74.651	0.028	77.398
41	0.019855	1.960	93.319	0.000	74.651	0.018	77.416
42	0.019599	0.002	93.320	0.178	74.829	0.000	77.416
43	0.019356	0.162	93.482	0.000	74.829	0.082	77.498
44	0.01911	0.000	93.482	0.253	75.083	0.000	77.498
45	0.018289	0.000	93.482	0.309	75.391	0.000	77.498
46	0.017945	0.003	93.485	0.000	75.391	0.002	77.500
47	0.017508	0.006	93.492	0.000	75.392	0.013	77.513
48	0.017306	0.000	93.492	0.420	75.811	0.000	77.513
49	0.016792	0.000	93.492	0.000	75.811	0.000	77.513
50	0.016067	0.000	93.492	0.000	75.811	0.009	77.523
51	0.015915	0.000	93.492	0.023	75.834	0.000	77.523
52	0.015451	0.000	93.492	0.003	75.837	0.000	77.523
53	0.015423	0.000	93.492	3.884	79.722	0.000	77.523
54	0.015406	0.000	93.492	0.490	80.211	0.000	77.523
55	0.015081	0.000	93.492	0.008	80.219	0.000	77.523
56	0.014968	0.000	93.492	0.407	80.626	0.000	77.523
57	0.01476	0.051	93.544	0.000	80.626	0.001	77.524
58	0.014682	0.001	93.544	0.007	80.633	0.000	77.524
59	0.014549	0.000	93.544	0.011	80.644	0.000	77.524
60	0.014488	0.001	93.546	0.000	80.644	0.000	77.524
61	0.014293	0.004	93.550	0.000	80.645	0.000	77.524
62	0.014192	0.698	94.248	0.157	80.802	0.001	77.524
63	0.014187	0.043	94.291	2.611	83.412	0.000	77.524
64	0.014032	0.000	94.291	0.025	83.438	0.000	77.524
65	0.013605	0.000	94.291	0.037	83.475	0.000	77.524
66	0.013411	0.020	94.312	0.021	83.496	0.001	77.525
67	0.013397	1.079	95.391	0.001	83.496	0.029	77.554
68	0.013392	0.003	95.393	0.047	83.543	0.000	77.555
69	0.013097	0.223	95.616	0.000	83.543	0.026	77.581
70	0.012897	0.000	95.616	0.001	83.544	0.000	77.581
71	0.012736	0.000	95.616	0.333	83.877	0.000	77.581
72	0.012717	0.000	95.617	0.000	83.878	0.000	77.581
73	0.012594	0.050	95.666	0.000	83.878	0.004	77.584

74	0.012379	0.000	95.666	0.103	83.980	0.021	77.605
75	0.01237	0.000	95.666	0.149	84.130	0.016	77.621
76	0.012126	0.154	95.820	0.000	84.130	0.370	77.991
77	0.011929	0.000	95.820	0.943	85.073	0.000	77.991
78	0.011734	0.000	95.820	0.069	85.142	0.002	77.993
79	0.011724	0.000	95.820	0.088	85.230	0.004	77.997
80	0.011567	0.001	95.822	0.000	85.230	1.893	79.890
81	0.011502	0.000	95.822	0.008	85.238	0.003	79.893
82	0.011288	0.005	95.827	0.007	85.245	0.600	80.493
83	0.011271	0.001	95.828	0.065	85.310	0.053	80.547
84	0.010965	0.008	95.835	0.000	85.310	1.798	82.344
85	0.010865	0.000	95.835	0.045	85.355	0.023	82.368
86	0.010853	0.023	95.859	0.000	85.355	2.133	84.500
87	0.010783	0.014	95.873	0.005	85.360	0.247	84.748
88	0.010778	0.002	95.875	0.043	85.404	0.035	84.783
89	0.01066	0.054	95.929	0.000	85.404	0.374	85.157
90	0.010605	0.000	95.929	0.000	85.404	0.000	85.157
91	0.010244	0.046	95.975	0.001	85.405	0.716	85.874
92	0.010236	0.000	95.975	0.079	85.484	0.005	85.879
93	0.010188	0.000	95.975	0.476	85.960	0.000	85.879
94	0.01012	0.009	95.984	0.000	85.960	0.024	85.904
95	0.010047	0.243	96.227	0.000	85.960	0.033	85.937
96	0.009927	0.082	96.309	0.006	85.967	0.000	85.937
97	0.009921	0.018	96.327	0.061	86.028	0.000	85.937
98	0.009903	0.603	96.930	0.000	86.028	0.012	85.949
99	0.009834	0.001	96.931	0.000	86.028	0.001	85.949
100	0.009772	0.000	96.931	0.176	86.204	0.000	85.950
101	0.009721	0.000	96.931	0.006	86.210	0.000	85.950
102	0.009662	0.005	96.935	0.001	86.211	0.068	86.018
103	0.009619	0.000	96.935	0.354	86.565	0.000	86.018
104	0.009565	0.000	96.936	0.000	86.565	0.044	86.062
105	0.009481	0.000	96.936	0.002	86.567	0.000	86.062
106	0.009458	0.000	96.936	0.000	86.567	0.014	86.076
107	0.009296	0.001	96.937	0.000	86.567	0.004	86.079
108	0.00928	0.000	96.937	0.000	86.567	0.000	86.080
109	0.009193	0.001	96.937	0.000	86.567	0.005	86.084
110	0.009071	0.000	96.937	0.061	86.628	0.000	86.085
111	0.009061	0.000	96.937	0.090	86.718	0.000	86.085
112	0.009004	0.000	96.937	0.036	86.755	0.000	86.085
113	0.008771	0.000	96.937	0.423	87.178	0.000	86.085
114	0.008767	0.003	96.940	0.070	87.248	0.001	86.086
115	0.008733	0.067	97.008	0.001	87.249	0.022	86.108
116	0.008654	0.003	97.011	0.110	87.359	0.004	86.112
117	0.008639	0.002	97.012	0.155	87.514	0.003	86.115

118	0.008547	0.000	97.012	0.059	87.573	0.000	86.115
119	0.008539	0.006	97.018	0.000	87.573	0.144	86.259
120	0.008413	0.000	97.018	0.001	87.574	0.003	86.261
121	0.008387	0.015	97.033	0.000	87.574	0.011	86.272
122	0.008282	0.000	97.033	0.000	87.574	0.104	86.376
123	0.008178	0.000	97.033	0.542	88.117	0.000	86.377
124	0.008105	0.001	97.035	0.002	88.119	0.127	86.504
125	0.008074	0.000	97.035	0.021	88.140	0.005	86.509
126	0.007948	0.064	97.099	0.001	88.141	0.010	86.519
127	0.007927	0.476	97.575	0.000	88.141	0.093	86.612
128	0.007731	0.000	97.575	0.029	88.170	0.000	86.612
129	0.007642	0.001	97.576	0.004	88.174	0.012	86.625
130	0.007555	0.007	97.583	0.000	88.174	0.230	86.855
131	0.007482	0.000	97.583	0.098	88.272	0.000	86.855
132	0.007422	0.031	97.614	0.000	88.273	0.150	87.004
133	0.00723	0.003	97.617	0.011	88.284	0.170	87.175
134	0.007208	0.000	97.617	0.422	88.706	0.006	87.181
135	0.00715	0.018	97.635	0.001	88.707	0.184	87.365
136	0.007066	0.006	97.642	0.001	88.707	0.001	87.366
137	0.006904	0.015	97.657	0.002	88.710	0.325	87.691
138	0.006877	0.000	97.657	0.192	88.902	0.006	87.696
139	0.00677	0.265	97.922	0.000	88.902	0.191	87.888
140	0.006677	0.000	97.922	0.002	88.904	0.417	88.305
141	0.006623	0.000	97.922	0.115	89.019	0.008	88.313
142	0.006424	0.005	97.927	0.001	89.019	0.968	89.281
143	0.006338	0.000	97.927	0.282	89.301	0.005	89.286
144	0.006316	0.069	97.997	0.000	89.301	0.562	89.849
145	0.006191	0.071	98.067	0.001	89.302	0.167	90.016
146	0.006088	0.094	98.162	0.004	89.306	0.264	90.280
147	0.006046	0.001	98.163	0.243	89.549	0.012	90.291
148	0.005929	0.032	98.194	0.001	89.550	0.531	90.823
149	0.005871	0.031	98.226	0.000	89.550	0.108	90.931
150	0.0058	0.000	98.226	0.344	89.894	0.001	90.932
151	0.005607	0.005	98.231	0.001	89.896	0.057	90.988
152	0.00553	0.089	98.319	0.000	89.896	0.002	90.990
153	0.005455	0.000	98.320	0.116	90.012	0.000	90.991
154	0.005367	0.175	98.495	0.000	90.012	0.042	91.032
155	0.005172	0.001	98.496	0.006	90.018	0.131	91.163
156	0.00513	0.000	98.496	0.178	90.195	0.006	91.168
157	0.004932	0.075	98.570	0.000	90.196	0.002	91.171
158	0.004889	0.004	98.574	0.003	90.198	0.157	91.327
159	0.004785	0.084	98.658	0.271	90.470	0.003	91.331
160	0.00478	0.087	98.746	0.251	90.721	0.013	91.344
161	0.00458	0.002	98.748	0.002	90.723	0.844	92.188

162	0.004451	0.000	98.748	1.274	91.998	0.013	92.201
163	0.004393	0.000	98.748	0.031	92.029	0.422	92.623
164	0.004346	0.175	98.924	0.000	92.029	0.006	92.629
165	0.00422	0.000	98.924	1.641	93.670	0.001	92.629
166	0.004023	0.135	99.059	0.001	93.670	0.018	92.648
167	0.003938	0.007	99.066	0.028	93.698	0.316	92.963
168	0.003905	0.000	99.066	0.542	94.240	0.020	92.983
169	0.003767	0.125	99.192	0.000	94.241	0.005	92.988
170	0.003692	0.010	99.201	0.002	94.242	0.810	93.798
171	0.003567	0.000	99.201	0.418	94.660	0.004	93.801
172	0.003484	0.131	99.332	0.001	94.661	0.054	93.856
173	0.003428	0.012	99.344	0.001	94.662	0.412	94.267
174	0.00319	0.010	99.354	0.301	94.963	0.003	94.271
175	0.003183	0.142	99.497	0.023	94.986	0.013	94.283
176	0.003024	0.005	99.502	0.001	94.987	0.443	94.726
177	0.002883	0.107	99.609	0.007	94.994	0.041	94.767
178	0.002871	0.004	99.613	0.245	95.239	0.000	94.768
179	0.002764	0.009	99.621	0.001	95.240	0.622	95.390
180	0.002559	0.094	99.715	0.000	95.240	0.035	95.424
181	0.002522	0.000	99.716	0.319	95.559	0.001	95.425
182	0.002453	0.003	99.719	0.001	95.559	0.539	95.964
183	0.00225	0.097	99.816	0.000	95.559	0.012	95.976
184	0.0021	0.001	99.816	1.560	97.119	0.043	96.020
185	0.002094	0.005	99.821	0.172	97.292	0.409	96.428
186	0.001958	0.102	99.923	0.000	97.292	0.024	96.452
187	0.001895	0.000	99.923	0.372	97.664	0.001	96.453
188	0.001804	0.005	99.927	0.000	97.664	0.493	96.946
189	0.001677	0.047	99.974	0.000	97.664	0.030	96.976
190	0.001477	0.006	99.980	0.000	97.664	0.404	97.380
191	0.001411	0.013	99.993	0.001	97.666	0.134	97.515
192	0.001407	0.000	99.993	1.072	98.737	0.001	97.515
193	0.001197	0.001	99.995	0.000	98.737	0.463	97.978
194	0.001145	0.005	100.000	0.000	98.737	0.071	98.049
195	0.001116	0.000	100.000	0.678	99.415	0.000	98.049
196	0.000873	0.000	100.000	0.003	99.418	0.114	98.163
197	0.000856	0.000	100.000	0.334	99.753	0.001	98.164
198	0.000806	0.000	100.000	0.000	99.753	1.683	99.847
199	0.000659	0.000	100.000	0.247	99.999	0.000	99.847
200	0.00065	0.000	100.000	0.000	100.000	0.153	100.000

APPENDIX-D

THE STANDARD SHAPE FUNCTOIN OF LUMPED MASS SYSTEM

TABLE-D THE STANDARD SHAPE FUNCTOINS FOR SEISMIC ANALYSIS WITH ELFM (CURTESY: ARMY OF CORPS OF ENGINEERS)

Displacements for step–tapered intake tower for first mode shape functions										
First shape Functions										
I_{top}/I_{base}	1.0	2.0	3.0	4.0	5.0	6.0	7.0	8.0	9.0	10
$Coef_x$ or $Coef_y$	3.091	5.391	7.391	9.194	10.86	12.41	13.88	15.27	16.6	17.87
Values of the shape function at the n^{th} node points (Φ_n)										
1.0L	1.0	1.0	1.0	1.0	1.0	1.0	1.0	1.0	1.0	1.0
0.9L	0.862	0.856	0.853	0.849	0.847	0.845	0.843	0.841	0.840	0.838
0.8L	0.725	0.714	0.706	0.701	0.696	0.692	0.689	0.685	0.683	0.680
0.7L	0.591	0.575	0.565	0.557	0.551	0.545	0.540	0.536	0.533	0.529
0.6L	0.461	0.443	0.431	0.422	0.415	0.409	0.404	0.400	0.396	0.392
0.5L	0.340	0.321	0.309	0.301	0.294	0.288	0.283	0.279	0.275	0.272
0.4L	0.230	0.214	0.204	0.197	0.191	0.186	0.182	0.179	0.176	0.173
0.3L	0.136	0.125	0.118	0.113	0.109	0.106	0.103	0.101	0.098	0.097
0.2L	0.064	0.058	0.054	0.051	0.049	0.048	0.046	0.045	0.044	0.043
0.1L	0.017	0.015	0.014	0.014	0.013	0.013	0.012	0.012	0.012	0.011
0.0L	0.0	0.0	0.0	0.0	0.0	0.0	0.0	0.0	0.0	0.0

APPENDIX-E

DETERMINATOIN OF MODAL PARTICIPATOIN FACTORS FOR ELFM

TABLE-E-1 THE MODAL PARTICIPATOIN FACTOR ALONG Y-AXIS FOR ELFM

The Total lumped mass at the nodes(m_{yr}) (KN- s^2/m)		Deflected Shape (Φ_{r-1})		$(m_{yr})*(\Phi_{r-1})$
m_{Y1}	805.06	Φ_{10-1}	1	805.060
m_{Y2}	1608.5	Φ_{9-1}	0.847	1362.400
m_{Y3}	1597.75	Φ_{8-1}	0.695	1110.436
m_{Y4}	1583.24	Φ_{7-1}	0.548	867.616
m_{Y5}	1561.74	Φ_{6-1}	0.407	635.628
m_{Y6}	1540.24	Φ_{5-1}	0.279	429.727
m_{Y7}	1486.49	Φ_{4-1}	0.167	248.244
m_{Y8}	1400.5	Φ_{3-1}	0.08	112.040
m_{Y9}	1271.5	Φ_{2-1}	0.022	27.973
m_{Y10}	1643.3	Φ_{1-1}	0	0.000
$L_{y1} = \sum_{0}^{L} m_{yr}\, \Phi_{r-1} =$				**5599.123**
$m_y^* =$ **3635.849**		$PF_{y1} = \frac{L_{y1}}{m_y^*} =$		**1.54**

TABLE-E-2 THE MODAL PARTICIPATOIN FACTOR ALONG X-AXIS FOR ELFM

The Total lumped mass at the nodes (m_{xr}) (KN- s^2/m)		Deflected Shape (Φ_{r-1})		$(m_{yr})*(\Phi_{r-1})$
m_{x1}	799.69	Φ_{10-1}	1	805.060
m_{x2}	1588.61	Φ_{9-1}	0.847	1362.400
m_{x3}	1572.49	Φ_{8-1}	0.695	1110.436
m_{x4}	1569.8	Φ_{7-1}	0.548	867.616
m_{x5}	1553.68	Φ_{6-1}	0.407	635.628
m_{x6}	1524.12	Φ_{5-1}	0.279	429.727
m_{x7}	1475.74	Φ_{4-1}	0.167	248.244
m_{x8}	1389.75	Φ_{3-1}	0.08	112.040
m_{x9}	1255.38	Φ_{2-1}	0.022	27.973
m_{x10}	1637.93	Φ_{1-1}	0	0.000
$L_{X1} = \sum_{0}^{L} m_{Xr}\, \Phi_{r-1} =$				**5541.198**
$m_X^* =$ **3597.00**		$PF_{X1} = \frac{L_{X1}}{m_X^*} =$		**1.54**

APPENDIX-F

DETERMINATOIN OF MODAL PARTICIPATOIN FACTORS FOR RSM

TABLE-F-1 THE MODAL PARTICIPATOIN FACTOR FOR EXCITATOIN ALONG X-AXIS FOR FIRST MODE

The Total lumped mass at the nodes (m_{xr}) (KN- s^2/m)		Deflected Shape (Φ_{r-1})		$(m_{yr})*(\Phi_{r-1})$
m_{x1}	799.69	Φ_{10-1}	1.000	805.06
m_{x2}	1588.61	Φ_{9-1}	0.866	1392.594
m_{x3}	1572.49	Φ_{8-1}	0.725	1158.101
m_{x4}	1569.8	Φ_{7-1}	0.591	935.0679
m_{x5}	1553.68	Φ_{6-1}	0.450	702.2589
m_{x6}	1524.12	Φ_{5-1}	0.322	496.1847
m_{x7}	1475.74	Φ_{4-1}	0.208	309.2697
m_{x8}	1389.75	Φ_{3-1}	0.114	159.7886
m_{x9}	1255.38	Φ_{2-1}	0.040	51.20134
m_{x10}	1637.93	Φ_{1-1}	0.000	0
$L_{X1} = \sum_{0}^{L} m_{Xr}\ \Phi_{r-1} =$				**6009.526**
m_x = **3597.00**		$PF_{X1} = \frac{L_{X1}}{m_x^*} =$		**1.517**

TABLE-F-2 THE MODAL PARTICIPATOIN FACTOR FOR EXCITATOIN ALONG X-AXIS FOR THIRD MODE

The Total lumped mass at the nodes (m_r) (KN-s2/m)		Deflected Shape (Φ_{r-1})		$(m_{xr})*(\Phi_{r-1})$
m_{x1}	799.69	Φ_{10-1}	1.000	799.69
m_{x2}	1588.61	Φ_{9-1}	0.485	770.7118
m_{x3}	1572.49	Φ_{8-1}	-0.030	-46.7076
m_{x4}	1569.8	Φ_{7-1}	-0.515	-808.214
m_{x5}	1553.68	Φ_{6-1}	-0.901	-1399.85
m_{x6}	1524.12	Φ_{5-1}	-1.139	-1735.38
m_{x7}	1475.74	Φ_{4-1}	-1.168	-1724.13
m_{x8}	1389.75	Φ_{3-1}	-0.970	-1348.47
m_{x9}	1255.38	Φ_{2-1}	-0.564	-708.482
m_{x10}	1637.93	Φ_{1-1}	0.000	0
$L_{X1} = \sum_{0}^{L} m_{Xr}\ \Phi_{r-1} =$				**-6200.84**
m_X = **3597.00**		$PF_{X1} = \frac{L_{X1}}{m_X^*} =$		**-0.72517**

APPENDIX-G

COMPARISON OF BASE SHEARS AND MOMENTS COMPUTATED BASED ON ACTUAL AND SIMPLIFIED CROSS-SECTOINS OF KESEM INTAKE TOWER

TABLE-G BASE SHEAR AND BASE MOMENTS OF ACTUAL AND SIMPLIFIESD SECTOINS

	Base Moments(MN-m)		Base shears(MN)	
	About X-X	About Y-Y	Along-X	Along-Y
Actual section	1738.472	1803.699	87.623	91.514
Simplified section	1656.435	1679.398	84.597	83.581
Differences (%)	4.7	6.9	3.45	8.66

APPENDIX-H

EXAMININATOIN OF IMPACT OF MODEL TYPE ON RSM ANALYSIS RESULTS

FIGURE-H-1 SHEAR FORCES COMPUTED WITH RSM FOR 3D AND BEAM-COLUMN MODELS

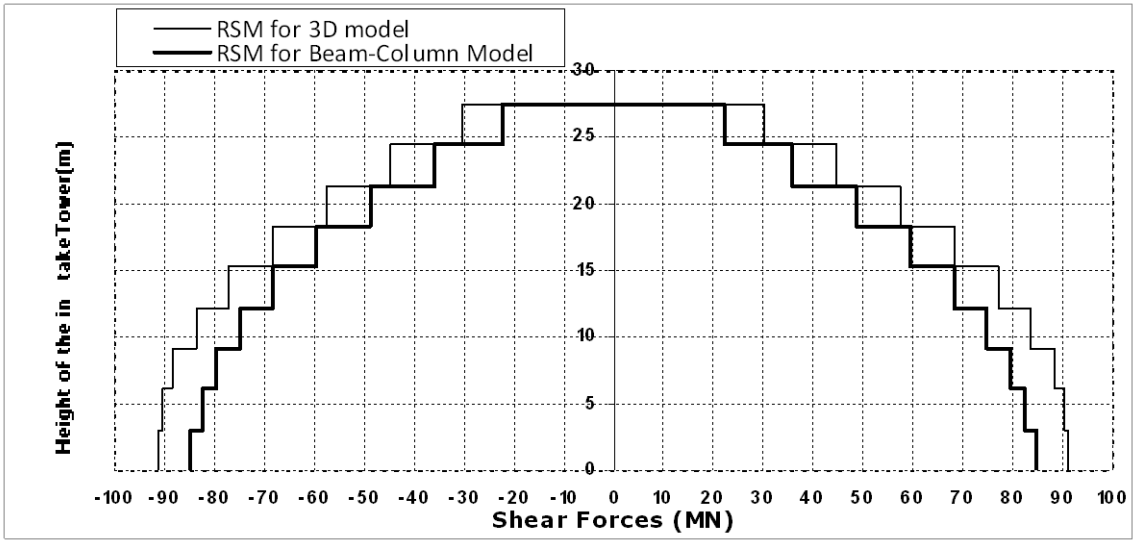

FIGURE-H-2 BENDING MOMENTS COMPUTED WITH RSM FOR 3D AND BEAM-COLUMN MODELS

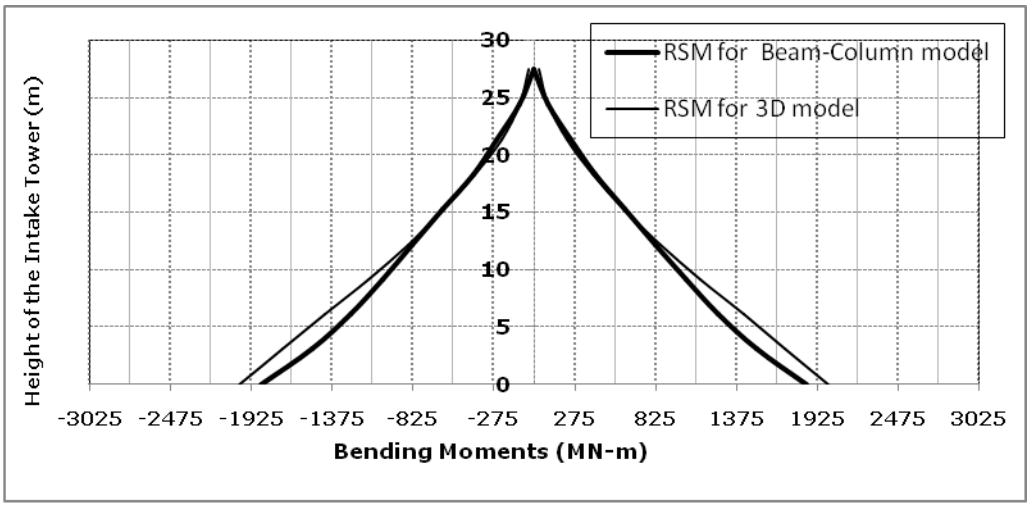

Bending Moment(MN-m)

TABLE-H BASE SHEAR AND BASE MOMENTS FOR BEAM-COLUMN AND 3-D MODELS

	Base Moments(MN-m)	Base shears(MN)
For Beam-Column model	1856.25	85
For 3-D model	2004.13	92
Differences (%)	7.4	7.6

APPENDIX-I

DIAGRAMATICAL COMPARISON BETWEEN ANALYSIS RESULTS COMPUTED WITH RSM AND MTHM FOR 3D MODEL

FIGURE-I SHEAR FORCES COMPUTED WITH RSM AND FOR 3D MODEL

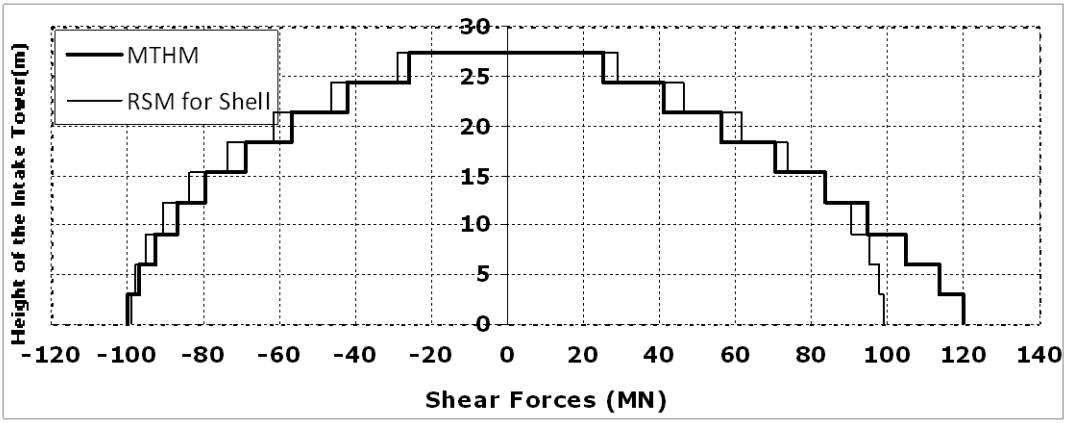

APPENDIX-J

SEISMIC ANALYSIS OF INTAKE TOWER BASED ON SIESMIC COEFFICIENT METHOD

Using Seismic Coefficient Method, the hydrodynamic pressures acting on surface of the intake tower were estimated based on its assumed parabolic distribution.

The pressure, along the parabolic, at any depth Z below water surface can be estimated with the following relation:-

$P_{ewh} = C_e \alpha_h \gamma_w Z$ (KN/m^2) and the resultant hydrodynamic load acting at o.4Z from bottom of the depth is given by:-

$p_{ewh} = C_e \alpha_h \gamma_w Z^2 B(\frac{Z}{Z_{max}})^2$ (KN), where

Φ_u the angle of inclination of up-stream face to the vertical,

C_e =dimensionless pressure factor, and is function of $\frac{Z}{Z_{max}}$,

α_h = Horizontal Seismic Coefficient,

γ_w =Unit weight of water,

B=Breadth of intake tower, and

Z_{max} =Maximum depth of water.

Indicative values of C_e are given in **Table-J-1** below.

TABLE-J-1 Seismic pressure factor, C_e (courtesy: **Novak et al (2007)**)

Ratio $\frac{Z}{Z_{max}}$	Pressure Factor, C_e	
	$\Phi_u=0^0$	$\Phi_u=15^0$
0.2	0.35	0.29
0.4	0.53	0.45
0.6	0.64	0.55
0.8	0.71	0.61
1.0	0.73	0.63

In addition to the hydrodynamic load, the pseudo-static inertia, acting at center of gravity, due to self–weight of a structure will be determined using the following relation:-

$p_{emh} = a_h p_{wh}$ Where,

p_{emh} = Load due to inertia, and

p_{wh} =Weight of the structure.

Based on the relations given above, the shear forces due to hydrodynamic and inertia loads acting at the base of the intake tower were computed along X and Y-Axes separately. After the separate computing, the total shear forces were obtained by summing the shear forces for inertia and hydrodynamic load along each axis. The results of the computations are summarized in Table-J-2 below

TABLE-J-2 Magnitude of shear forces computed at base of the intake tower using SCM.

Sources of the Shear Forces	Magnitude of the Shear Forces(MN)	
	Along X-Axis	Along Y-Axis
Hydrodynamic load	11.16	8.73
Inertia of the intake tower	24.38	24.38
Total Shear Forces=	35.38	33.11

In same manner, the bending moment due to the hydrodynamic and inertial loads were calculated separately for each axis. The moments were calculated by multiplying previously calculated shear forces by their respective moment arm lengths. Finally, in order to get the total moments, the moments of hydrodynamic and inertia loads were summed as shown in Table-J-3 below.

TABLE-J-3 shear forces computed at base of the intake tower using SCM.

Sources of the Bending Moments	Magnitude of the Bending Moments(MN-m)	
	About X-X	About Y-Y
Hydrodynamic load	95.91	122.61
Inertia of the intake tower	334.593	334.593
Total Bending Moments =	457.21	430.50